



HAL
open science

Reef response to sea-level and environmental changes in the Central South Pacific over the past 6,000 years

N. Hallmann, G Camoin, Anton Eisenhauer, Elias Samankassou, Claude Vella, Alain Botella, G.A. Milne, Virginie Pothin, Philippe Dussouillez, Jules Fleury, et al.

► To cite this version:

N. Hallmann, G Camoin, Anton Eisenhauer, Elias Samankassou, Claude Vella, et al.. Reef response to sea-level and environmental changes in the Central South Pacific over the past 6,000 years. *Global and Planetary Change*, 2020, 195, pp.103357. 10.1016/j.gloplacha.2020.103357 . hal-03435146

HAL Id: hal-03435146

<https://hal.science/hal-03435146>

Submitted on 18 Nov 2021

HAL is a multi-disciplinary open access archive for the deposit and dissemination of scientific research documents, whether they are published or not. The documents may come from teaching and research institutions in France or abroad, or from public or private research centers.

L'archive ouverte pluridisciplinaire **HAL**, est destinée au dépôt et à la diffusion de documents scientifiques de niveau recherche, publiés ou non, émanant des établissements d'enseignement et de recherche français ou étrangers, des laboratoires publics ou privés.



Distributed under a Creative Commons Attribution - NonCommercial - NoDerivatives 4.0 International License

1 **Reef response to sea-level and environmental changes in the Central South Pacific over**
2 **the past 6,000 years**

3

4 Hallmann, N.^{a*}, Camoin, G.^a, Eisenhauer, A.^b, Samankassou, E.^c, Vella, C.^a, Botella, A.^d,
5 Milne, G.A.^d, Pothin, V.^a, Dussouillez, P.^a, Fleury, J.^a, Fietzke, J.^b, Goepfert, T.^c

6

7 ^a Aix-Marseille Université, CNRS, IRD, INRAE, Coll France, CEREGE, Europôle
8 Méditerranéen de l'Arbois, BP80, 13545 Aix-en-Provence cedex 4, France

9 ^b GEOMAR Helmholtz-Zentrum für Ozeanforschung Kiel, Wischhofstraße 1-3, 24148 Kiel,
10 Germany

11 ^c University of Geneva, Department of Earth Sciences, Rue des Maraîchers 13, CH-1205
12 Geneva, Switzerland

13 ^d University of Ottawa, Department of Earth and Environmental Sciences, Ottawa, Ontario
14 K1N 6N5, Canada

15 ^e Arizona State University, School of Earth & Space Exploration, 550 E Tyler Mall, Tempe,
16 AZ 85287-1404, USA

17

18

19

20

21

22

23

24

25 * Corresponding author: hallmann@cerege.fr

26

27 **Abstract**

28 Geological records of coastal system evolution during past higher and/or rising sea levels
29 provide an important baseline for developing projections regarding the response of modern
30 coastal systems to future sea-level rise. The mid-late Holocene corresponds to the most recent
31 window into natural variability prior to the Anthropocene and involves slow-rate and low-
32 amplitude sea-level changes that were mostly governed by a limited glacio-eustatic
33 contribution, most likely sourced from Antarctica, and ‘glacial isostatic adjustment’
34 processes.

35 This paper documents in unprecedented detail the response of coral reefs and coastal systems
36 to changing accommodation space in relation to mid-late Holocene sea-level changes in
37 French Polynesia.

38 The sea-level curve that underpins this study has a global significance and documents a single
39 short-lived sea-level highstand between 4.10 and 3.40 kyr BP. The amplitude of the highstand
40 is less than one metre, within the range of the predicted sea level at the end of the current
41 century. The reported relative sea-level changes are characterized by slow rates ranging from
42 a few tens of millimetres per year to up to 2.5 mm/yr and by significant sea-level stability
43 (stillstands) lasting more than a century and up to 250 years, defining a step-like pattern. Sea-
44 level variability probably driven by climatic oscillations on interannual to millennial time
45 scales is evidenced during the entire time window.

46 The detailed reconstruction of reef development over the last 6,000 years brings valuable
47 information regarding coral reef dynamics and coastal processes during periods of higher sea
48 level and wave energy regimes. The persistence of stable and optimal depositional
49 environments over the last 6,000 years is demonstrated by the constant overall composition
50 and diversity of reef communities and the almost continuous development of coral
51 microatolls. The facies distribution as well as the lateral extension and shift of facies belts
52 have been governed by variations in accommodation space, which are controlled by relative

53 sea-level changes and antecedent topography. The widespread development of mid-late
54 Holocene reef deposits in coastal areas suggests that they have played a prominent role in
55 global processes related to the formation and shaping of modern islands.

56

57 **Keywords**

58 *Porites* microatolls; mid-late Holocene sea level; U-series dating; French Polynesia; low-lying
59 islands; storm deposits

60 **1. Introduction**

61 One of the most societally relevant objectives of research in the Earth Sciences is to better
62 understand past environmental changes to enable future projections with improved accuracy.
63 Increasing atmospheric pCO₂ is expected to be the main driving force for future climatic
64 changes, of which sea-level rise and changes in the hydrological cycle are among the most
65 pressing issues for coastal societies. Over the past few decades, most of the measured global
66 mean sea-level rise (i.e., 3.5 mm/yr since the early 1990s; Church et al., 2013) has been
67 ascribed to the melting of polar ice caps and the thermal expansion of the ocean in response to
68 global warming. Global mean sea level is expected to rise between 0.5 and 1.5 m by the year
69 2100 as a consequence of warming from greenhouse gas forcing (Alley et al., 2007; Church et
70 al., 2013; IPCC, 2018). Such a rise in sea level would have severe impacts on coastal
71 ecosystems, water supplies and densely populated coastal areas in the Low-Elevation Coastal
72 Zone (McGranahan et al., 2007; Kekeh et al., 2020), especially on low-lying islands, which
73 stand less than 3 m above mean sea level. However, projections of sea-level rise remain
74 highly uncertain, primarily due to our poor understanding of the sensitivity of ice sheets to
75 sustained warming (IPCC, 2018) and, accordingly, the future evolution of coastal systems
76 cannot be accurately predicted.

77 The future response of shorelines to rising sea level can be evaluated based on high-resolution
78 studies of geological analogues involving past periods of higher and/or rising sea level
79 characterized by slow-rate, low-amplitude and high-frequency relative sea-level (RSL)
80 changes (see Camoin and Webster, 2015 and references therein). Investigating Holocene
81 analogues to evaluate future sea-level scenarios is a common approach (e.g., Woodroffe and
82 Murray-Wallace, 2012; Helfensdorfer et al., 2019). The mid-late Holocene represents the
83 most recent period characterized by a higher than present sea level. Responses of coral reefs
84 and coastal systems to RSL changes, including changes in sedimentation patterns and island
85 development, during this time window are of global significance. However, so far, these

86 processes have been scarcely documented in the mid-late Holocene (Hopley, 1982; Hopley et
87 al., 2007; Harris et al., 2015), and nowhere near at the temporal and spatial resolutions that are
88 needed to better predict the future evolution of coastal systems, especially coral reefs.
89 Furthermore, the impact of mid-late Holocene RSL changes and other environmental factors
90 on reef architecture and composition remains poorly resolved (Camoin and Webster, 2015).
91 These are key aspects of this study.

92 Mid-late Holocene RSL changes were mostly governed by a limited glacio-eustatic
93 contribution and ‘glacial isostatic adjustment’ (GIA) processes (e.g., Camoin and Webster,
94 2015 and references therein). At ‘far-field’ sites, the ‘equatorial ocean syphoning’ (Mitrovica
95 and Peltier, 1991; Mitrovica and Milne, 2002) and hydro-isostasy are generally the key
96 processes that result in and control the timing and amplitude of sea-level highstands of a few
97 decimetres to about a metre, similar in amplitude to the sea-level rise that is expected before
98 the end of the current century (Alley et al., 2007; Church et al., 2013; IPCC, 2018). GIA
99 processes display significant spatial variability (Milne and Mitrovica, 2008; Lambeck et al.,
100 2010) that induces regional disparities in mid-late Holocene RSL changes (Milne et al., 2009;
101 Camoin and Webster, 2015) and hence in reef development histories.

102 Given the spatial variability in Holocene RSL, detailed regional studies are, in general,
103 necessary to constrain accurately the timing and amplitude of the mid-late Holocene RSL
104 changes and to evaluate their impact on coral reef growth and the evolution of coastal systems
105 during this time window.

106 Among sea-level indicators that are used to reconstruct mid-late Holocene RSL changes, coral
107 microatolls represent unique archives of the mean low water springs (MLWS) level in open
108 water settings. Their accurate dating by multiple techniques (e.g., ^{14}C , U-series; see Camoin
109 and Webster, 2015) allows them to be used to track the evolution of MLWS through time, as
110 well as regional sea-level trends and climatic oscillations on interannual to millennial time
111 scales (Hallmann et al., 2018). Their vertical growth is constrained by exposure at lowest tides

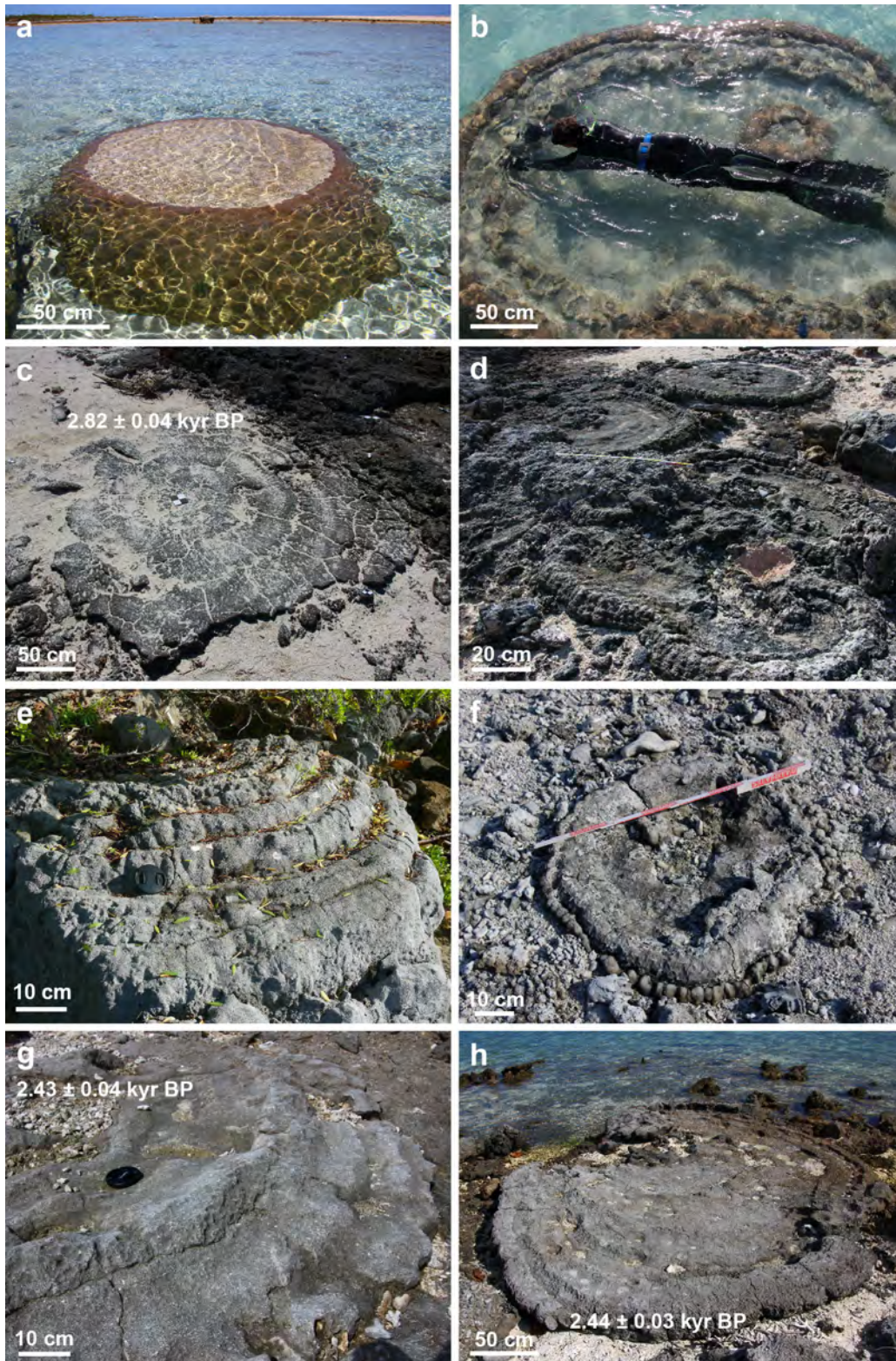
112 (Smithers and Woodroffe, 2000; Hopley et al., 2007; Meltzner and Woodroffe, 2015), which
113 is reflected by their overall flat dead upper surface (Fig. 1a-c; ‘microatoll plane’) and their
114 lateral growth. In addition, the upper surface of coral microatolls reflects subtle sea-level
115 changes. A rise in sea level is indicated by a higher outer margin compared to the central
116 depression, as well as overgrowths along the outer margin and/or on top of the former coral
117 colony that may record a time elapse between two periods of coral growth (Fig. 1d). On the
118 contrary, a sea-level fall is typified by the occurrence of a lower margin compared to the
119 central part (Fig. 1e-g). A more complex microtopography of the upper surface of coral
120 microatolls may include a succession of ridges and overgrowths (Fig. 1h), up to 20 cm high,
121 that reflect sea-level variations on decadal to sub-decadal time scales.

122 The Central South Pacific, especially French Polynesia, is an ideal region for palaeo-sea-level
123 studies targeted at understanding environmental drivers of sea-level change. This is due to its
124 location in the ‘far-field’ as well as the latitudinal distribution of its islands and their tectonic
125 stability and/or well constrained subsidence rates during deglacial and postglacial periods
126 (Camoin et al., 2012; Deschamps et al., 2012). This paper documents, in unprecedented detail
127 and at high resolution, the responses of coral reefs and coastal systems to mid-late Holocene
128 RSL changes in this region by focusing on microatoll fields and reef flat areas that are at or
129 near sea level. It provides the opportunity to better assess how these systems might respond to
130 low-amplitude (~1 m) sea-level changes that are expected before the end of the current
131 century (Alley et al., 2007; Church et al., 2013; IPCC, 2018).

132

133

134



135

136 Fig. 1. *Porites* microatolls. (a) and (b) Modern microatolls (Makemo, Fakarava). (c)
 137 Microatoll with a flat surface indicating a stable sea level (SL) for about 150 years (Bora
 138 Bora). (d) Field of microatolls with a higher margin reflecting a SL rise during their growth
 139 (Maupiti). (e) Microatoll with a lower margin indicating a SL fall during its growth

140 (Fakarava). (f) Microatoll exhibiting late overgrowth along its margin (Bora Bora). (g)
141 Microatoll with a lower margin indicating a SL fall during its growth and ridges on its
142 surface typifying low-amplitude, high-frequency SL changes (Bora Bora). (h) Microatoll
143 displaying ridges on its upper surface reflecting low-amplitude, high-frequency SL changes
144 (Bora Bora).

145

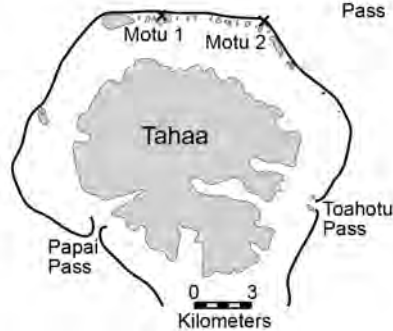
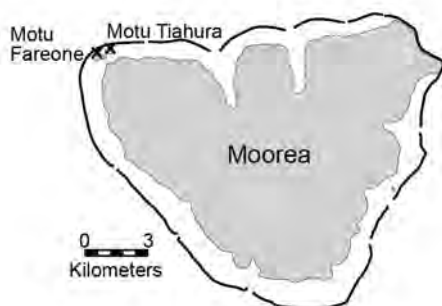
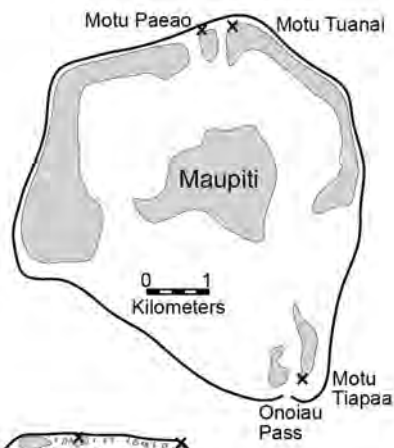
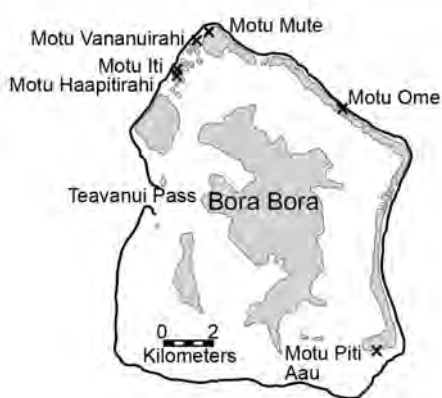
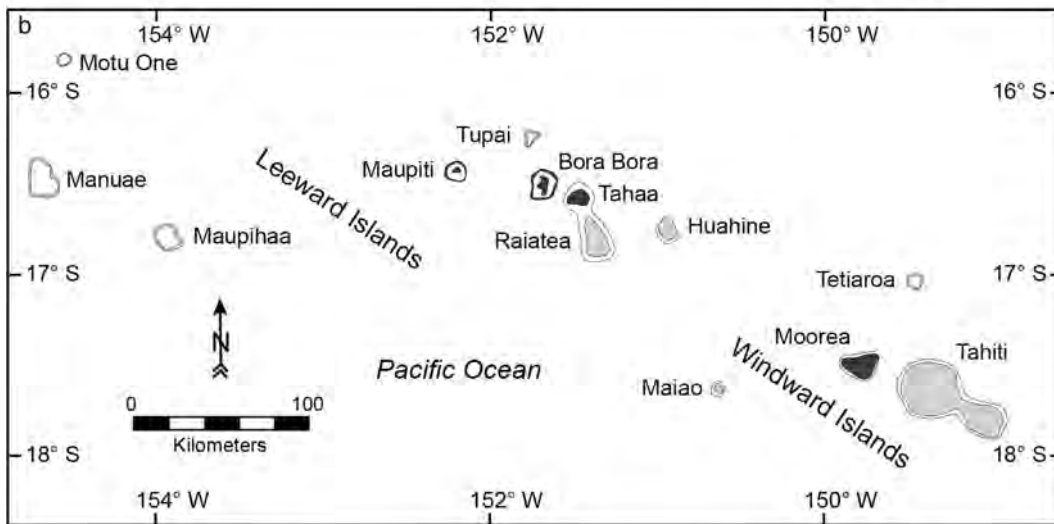
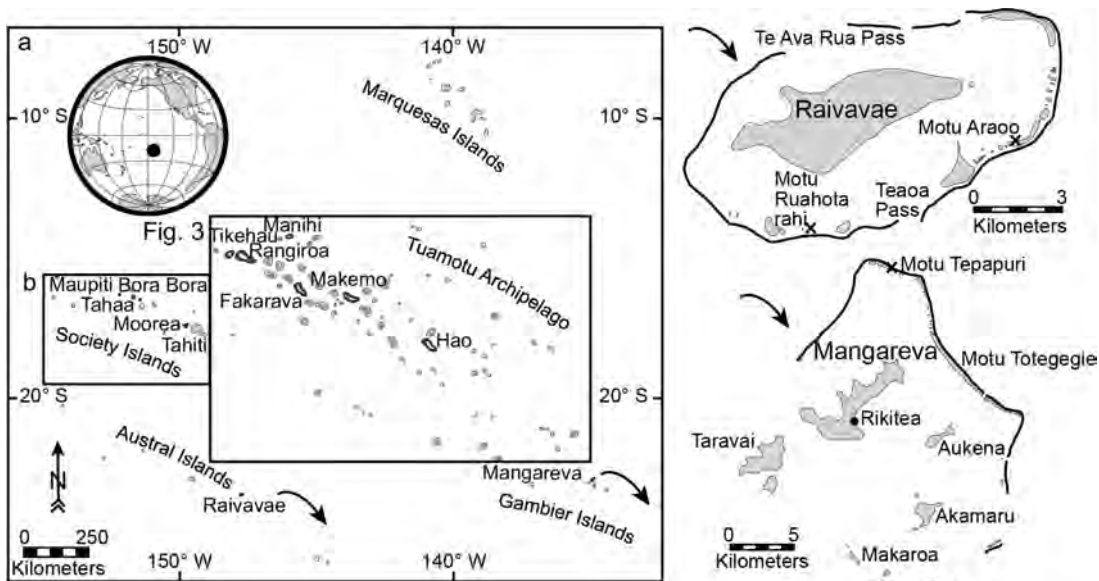
146 **2. Setting**

147 *2.1. Regional and climatic settings*

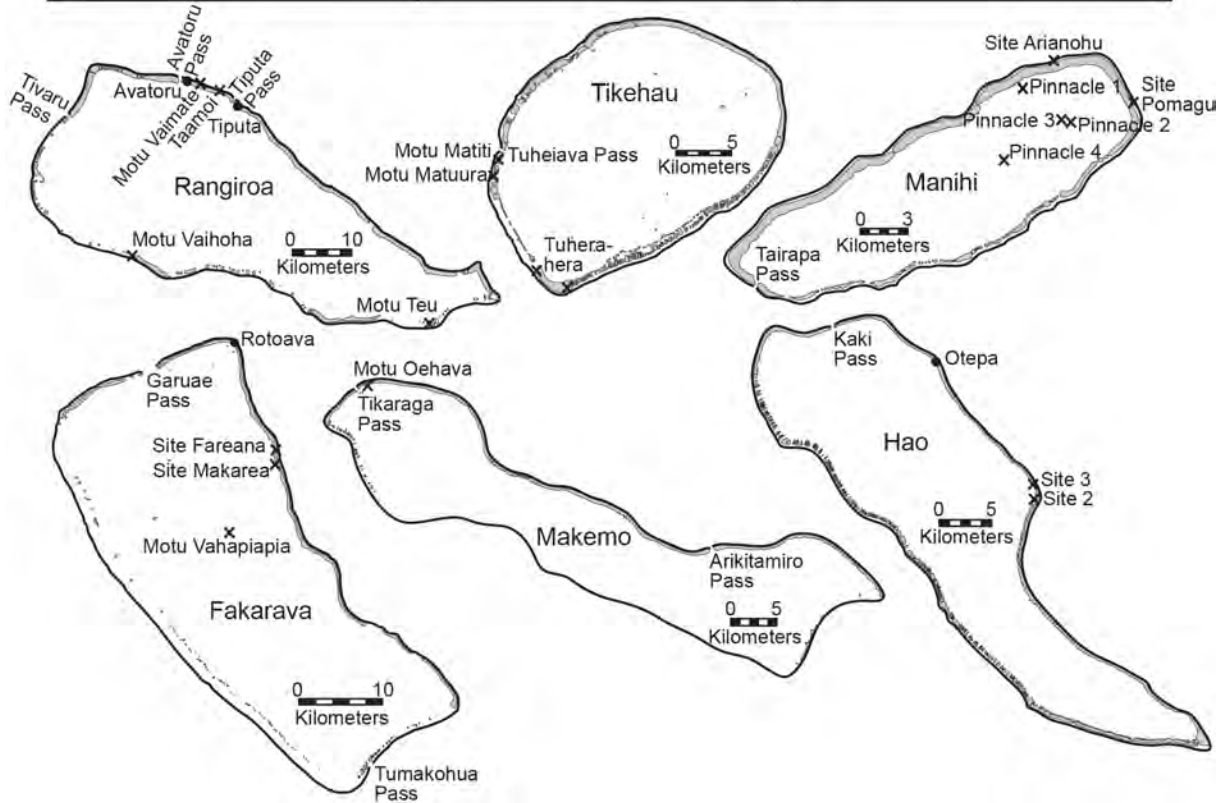
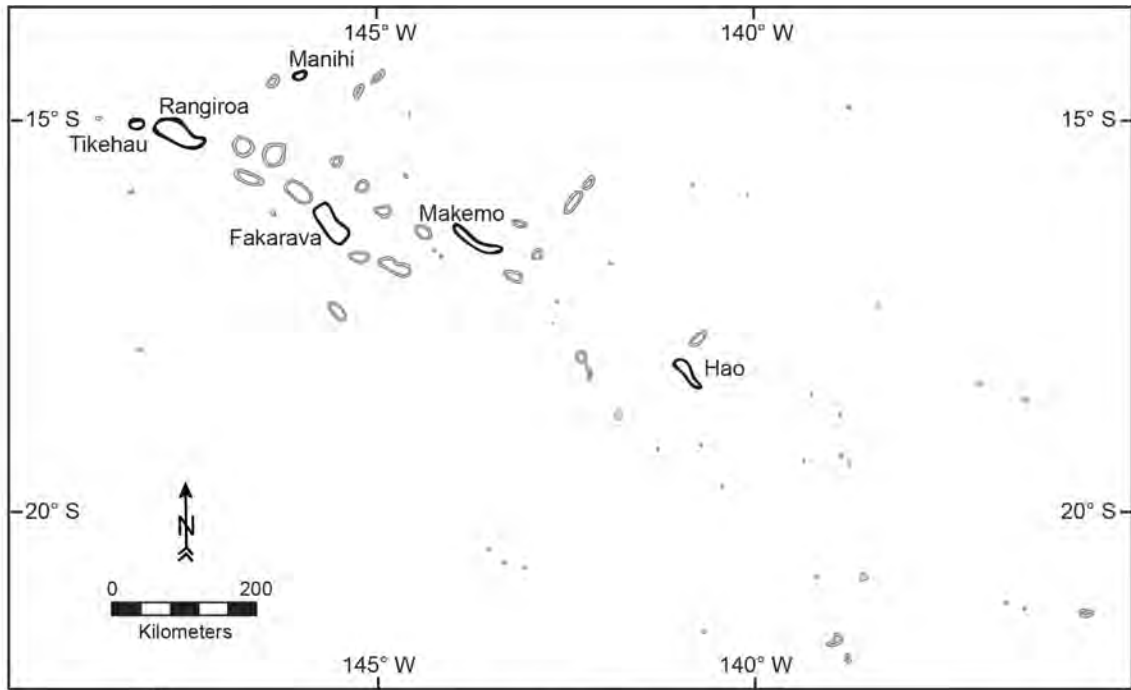
148 French Polynesia covers a vast oceanic region located in the Central South Pacific. It includes
149 83 atolls or low-lying islands and 35 high volcanic islands that form five archipelagos
150 dispersed along a general NW-SE axis: Society, Tuamotu, Austral, Marquesas and Gambier
151 (Fig. 2). French Polynesian reef systems are comprised of oceanic reefs developed on atolls,
152 banks and high islands.

153 The twelve islands that were investigated during this study cover a wide range of latitudes and
154 longitudes (S14°20' to S23°54', W152°18' to W134°50'). They are distributed in the Society
155 Archipelago (Moorea, Bora Bora, Maupiti and Tahaa), in the Tuamotu Archipelago
156 (Makemo, Manihi, Tikehau, Rangiroa, Fakarava and Hao), in the Austral Islands (Raivavae)
157 and Gambier Islands (Figs. 2, 3). The location of our study sites on these islands are indicated
158 in Figure 2. In addition, three other high islands, Raiatea and Tahiti (Society Archipelago) and
159 Tubuai (Austral Islands) were explored, but no sampling was carried out.

160



162 Fig. 2. Map of French Polynesia. (a) Islands have been studied in four archipelagos: Society,
163 Tuamotu (see details in Fig. 3), Austral and Gambier Islands. The two black arrows direct to
164 detailed maps of Raivavae and Mangareva. (b) Map of the Society Islands with studied
165 islands in black and detailed maps of the four studied islands in this archipelago below.
166 Motus in grey, barrier reef as black lines and study sites are indicated by crosses.
167



168

169 Fig. 3. Map of the Tuamotu Archipelago and detailed maps of the studied atolls in this
 170 archipelago.

171

172 The climate in French Polynesia is tropical and humid and includes two distinct seasons: a
 173 warm and rainy season from November to April and a cool and relatively dry season from

174 May to October (see details in Gabrié and Salvat, 1985; Galzin and Pointier, 1985; Harmelin-
175 Vivien, 1985).

176 French Polynesia is in the trade-wind zone. The dominant winds generally blow from the N
177 and NE, except from May to October when they blow from the SE. There are long periods of
178 calm from April to June. Tropical cyclones may come both from the NE and the NW from
179 November to April and are generally rare, from one to three per century in the Marquesas, the
180 northern Tuamotus and the Austral Islands to four to eight per century in a region extending
181 from the Tuamotus to the Gambier Islands, through the Society Islands. However, some years,
182 such as in 1982-1983, have been characterized by an exceptional high number of cyclones,
183 eight in total (Gabrié and Salvat, 1985).

184 The tidal amplitude is low on French Polynesian islands and ranges from 0.15 m on the
185 Society Islands up to 0.5 m on the Gambier Islands (Hallmann et al., 2018).

186 Based on sparsely distributed tide gauge records and shorter gridded sea level fields
187 based on satellite altimetry data and outputs of two numerical ocean models, it has been
188 demonstrated that in French Polynesia, the climate-related sea level rose at an average rate of
189 2.4 mm/yr significantly faster (40%) than the mean global mean rate (of about 1.7 mm/yr)
190 over the 1950-2010 time span (Meysignac et al., 2012).

191

192 *2.2. Geological setting*

193 French Polynesian islands are distributed along five linear, subparallel chains that were
194 created by volcanic processes driven by stationary hot spots from the Paleocene to the
195 present: Mehetia (Society), McDonald Seamount (Cook-Austral), Fatu-Hiva (Marquesas) and
196 Pitcairn (Gambier-Tuamotu; see e.g., Duncan and McDougall, 1974, 1976). Tectonic
197 movements affecting Polynesian islands are related to the volcanic evolution of the region.
198 The Society islands experienced a slow and regular subsidence during the Late Pleistocene
199 and the Holocene, especially due to the cooling and the concomitant sinking of aging

200 lithosphere (Blais et al., 2000; Guillou et al., 2005; Yamamoto et al., 2007; Neall and
201 Trewick, 2008). Subsidence rates of 0.25 mm/yr have been estimated for Tahiti based on drill
202 core data (Bard et al., 1996; Camoin et al., 2012; Deschamps et al., 2012), while a rate of 0.15
203 \pm 0.15 mm has been deduced from five independent geophysical measurements (Fadil et al.,
204 2011). Subsidence rates for Bora Bora have been estimated to 0.05 to 0.14 mm/yr, based on
205 drill core data (Gischler et al., 2016), while subsidence rates of less than 0.05 mm/yr can be
206 assumed for Maupiti, which is located 45 km west of Bora Bora and thus further away from
207 the Mehetia active hot spot. Subsidence rates for the Tuamotus are assumed to be of 0.01
208 mm/yr, based on the cooling of Miocene volcanoes (Jarrard and Clague, 1977; Parsons and
209 Sclater, 1977; Detrick and Crough, 1978; Schlanger et al., 1984; Duncan and Clague, 1985).
210 Some northern Tuamotu islands, e.g., Anaa (Pirazzoli et al., 1988) and Makatea (Montaggioni
211 and Camoin, 1997) have been uplifted as the result of the loading of the Tahiti and Moorea
212 volcanic systems (Lambeck, 1981). The coeval uplift rates for Rangiroa and Tikehau, which
213 are located approximately 80 km north of Makatea, have been less than 0.05 mm/yr, but led to
214 the exposure of *feos* (= fossil reef deposits) of up to 2 m and 6 m high for Rangiroa and
215 Tikehau, respectively. Fakarava, Manihi, Makemo and Hao, which are located between 400
216 km and 850 km away from Tahiti were too far to be affected by the loading of the Tahiti and
217 Moorea volcanic systems. Subsidence rates of the southern Tuamotus, including the Gambier
218 Islands, are assumed to be of 0.03 mm/yr, based on the cooling of late Miocene and Pliocene
219 volcanoes related to the Pitcairn hot spot (Brousse et al., 1972; Guillou et al., 1994). The 2000
220 km long Cook-Austral volcanic chain is aligned in a NW-SE direction and reveals a complex
221 geological history with islands originating from different hot spots and subsidence rates of the
222 Austral Islands are assumed to be of 0.03 mm/yr (e.g., Duncan and McDougall, 1976; McNutt
223 et al., 1997; Clouard and Bonneville, 2001; Bonneville et al., 2002, 2006).

224

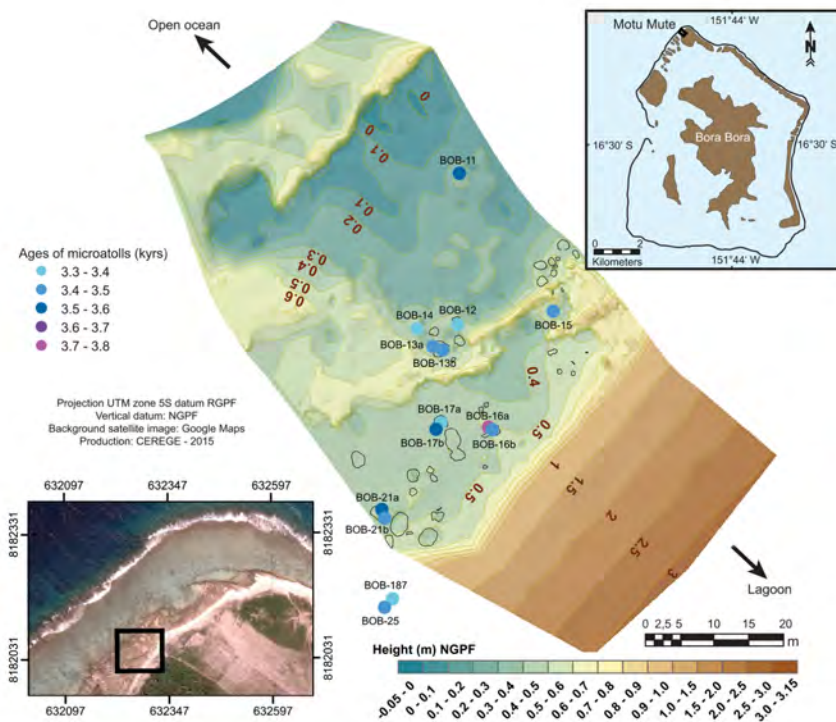
225 **3. Material and Methods**

226 The present study is based on field studies, high-precision GPS positioning and surveying, as
227 well as a chronological study of all components of mid-late Holocene coral reef systems.

228 All collected samples of coral colonies and associated sediments were cut with a rock saw and
229 subsequently studied with regard to sedimentology, including the reconstruction of
230 depositional environments, petrography and carbonate diagenesis. Thin sections were
231 qualitatively studied under a polarization microscope. Corals were identified at the lowest
232 taxonomic level possible using the standard publications of Wallace (1999), Veron (2000) and
233 Humblet et al. (2015). Snorkel trips around the study sites were undertaken to collect
234 qualitative data regarding bottom characteristics and modern reef assemblages to be compared
235 to their mid-late Holocene counterparts.

236 Radiometric U-series ages have been obtained from *in situ* coral microatolls and *in situ* coral
237 colonies that are associated to microatolls or occurring in reef flat units, and have been used to
238 reconstruct RSL changes. In addition, reworked coral colonies that form the bulk of
239 conglomerate units and reef boulders have been dated to further unravel the mid-late
240 Holocene development of reef systems. Overall, 305 pristine coral samples, showing an
241 average aragonite content of 97.6% (see details in Hallmann et al., 2018), were dated by U-
242 series measurements performed at the GEOMAR (Kiel, Germany) using a Thermo Fisher
243 Neptune multi-ion-counting inductively coupled plasma mass spectrometer (MC-ICP-MS).
244 The chemical preparation, dating procedures and the age calculation are described in Fietzke
245 et al. (2005) and Hallmann et al. (2018). Seventy-eight samples from 72 microatolls
246 represented the database on which the mid-late Holocene sea-level curve has been initially
247 reconstructed (Hallmann et al., 2018). Thirteen samples from six additional microatolls, 84
248 samples of *in situ* corals in reef flat units, 48 coral samples from conglomerates have been
249 dated for the current study, in addition to 20 samples from reef boulders (Supplementary
250 Tables 1 and 2).

251 The methods used for acquiring and processing GPS data are described in Hallmann et al.
252 (2018). Mid-late Holocene RSL changes have been reconstructed using two methods
253 (Hallmann et al., 2018): 1) The definition of a biological elevation reference for each study
254 site allowed to compare directly the elevations of fossil and modern microatolls to deduce
255 relative sea-level changes, and 2) the GPS measurements of dated microatolls referenced to
256 the RGPF (geodetic datum in French Polynesia) associated with the NGPF (vertical datum),
257 which is a semi-dynamic system that is especially based on sites equipped with DORIS
258 (Doppler Orbitography by Radiopositioning Integrated by Satellite) stations. In this study,
259 dated reef flat units have been referenced to RGPF and NGPF to be directly compared to the
260 distribution of microatolls. The elevations of dated coral colonies, including microatolls,
261 have been corrected for subsidence. Rates of sea-level changes have been calculated based
262 on the age and elevation differences between two successive coral microatolls with reference
263 to the elevation of modern microatolls. These rates therefore reflect changes in MLWS level
264 throughout the mid-late Holocene. Uncertainties related to measurements of microatoll
265 elevation are of ± 2 cm and uncertainties concerning their ages are of 1% or less of the
266 measured ages. In addition to GPS positioning of samples, high-resolution maps and
267 transects were generated using ArcGIS 10.1 (Fig. 4) and structure-from-motion
268 photogrammetry was used to produce high-resolution 3D topographic maps (Fig. 5).

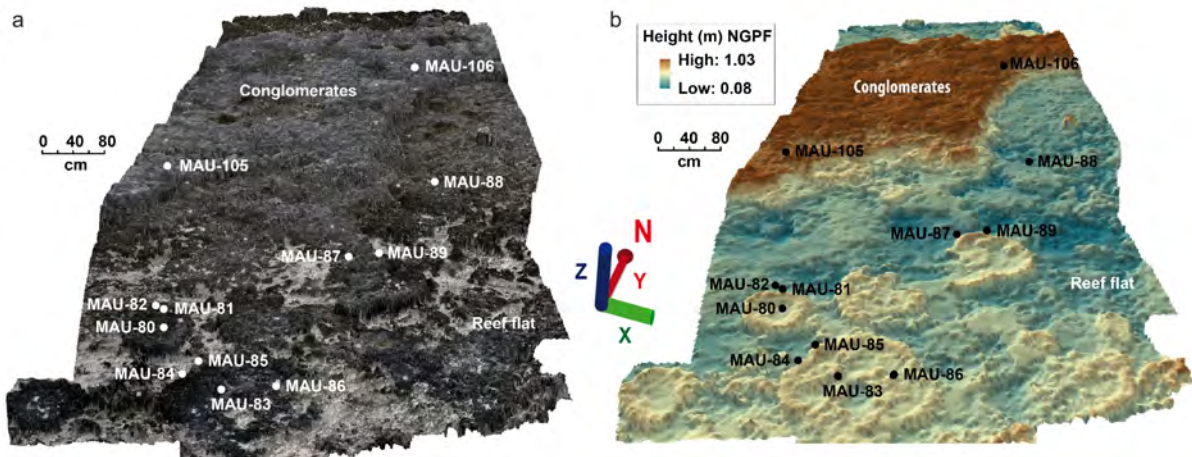


269

270 Fig. 4. High-resolution map of the Bora Bora study site on Motu Mute. Map of Bora Bora
 271 shows the location of Motu Mute and the black box on Motu Mute indicates the mapped
 272 area. The more detailed inset map shows the location of the mapped area (black box) close
 273 to the airstrip on Motu Mute. Circles on the high-resolution map indicate position and ages
 274 of *Porites* microatoll samples. Fields of microatolls are located on the Holocene reef flat and
 275 are partly covered by conglomerates. Elevations are based on NGPF measurements
 276 (geodetic datum in French Polynesia).

277

278



279

280 Fig. 5. Photogrammetry of a study site on Maupiti (Motu Tuanai). 3D reconstruction with

281 (a) photographic texture and (b) coloured texture indicating heights. *Porites* microatolls

282 overlay Holocene reef flat units and are partly covered by conglomerates. Circles indicate

283 the sample positions. The scale changes due to the perspective view. Agisoft Photoscan

284 Professional version 1.2 was used to produce the 3D model. Elevations are based on NGPF

285 measurements (geodetic datum in French Polynesia).

286

287

288 4. Results

289 4.1. Mid-late Holocene reef sequence

290 In the following text, current elevations and depths measured in the field refer to present mean

291 sea level. For microatolls, reference to modern MLWS is indicated when appropriate.

292 In the studied islands, the mid-late Holocene reef sequence generally forms the transition

293 between modern beach deposits and reef environments, including lagoonal and reef flat areas

294 (Fig. 6), from about 4 m deep to 2 m high. This reef sequence occurs at various elevations on

295 the ocean sides of *motus* (Gabrié and Salvat, 1985; Pirazzoli et al., 1985, 1988; Pirazzoli and

296 Montaggioni, 1988; Rashid et al., 2014; Hallmann et al., 2018), which are small vegetated

297 islets and sand cays that are located on barrier reef systems. A large number of narrow,

298 shallow waterways called *hoas* are located on the reef rim between elongated *motus* and
299 connect permanently or temporarily the lagoon with the ocean (Fig. 6).

300

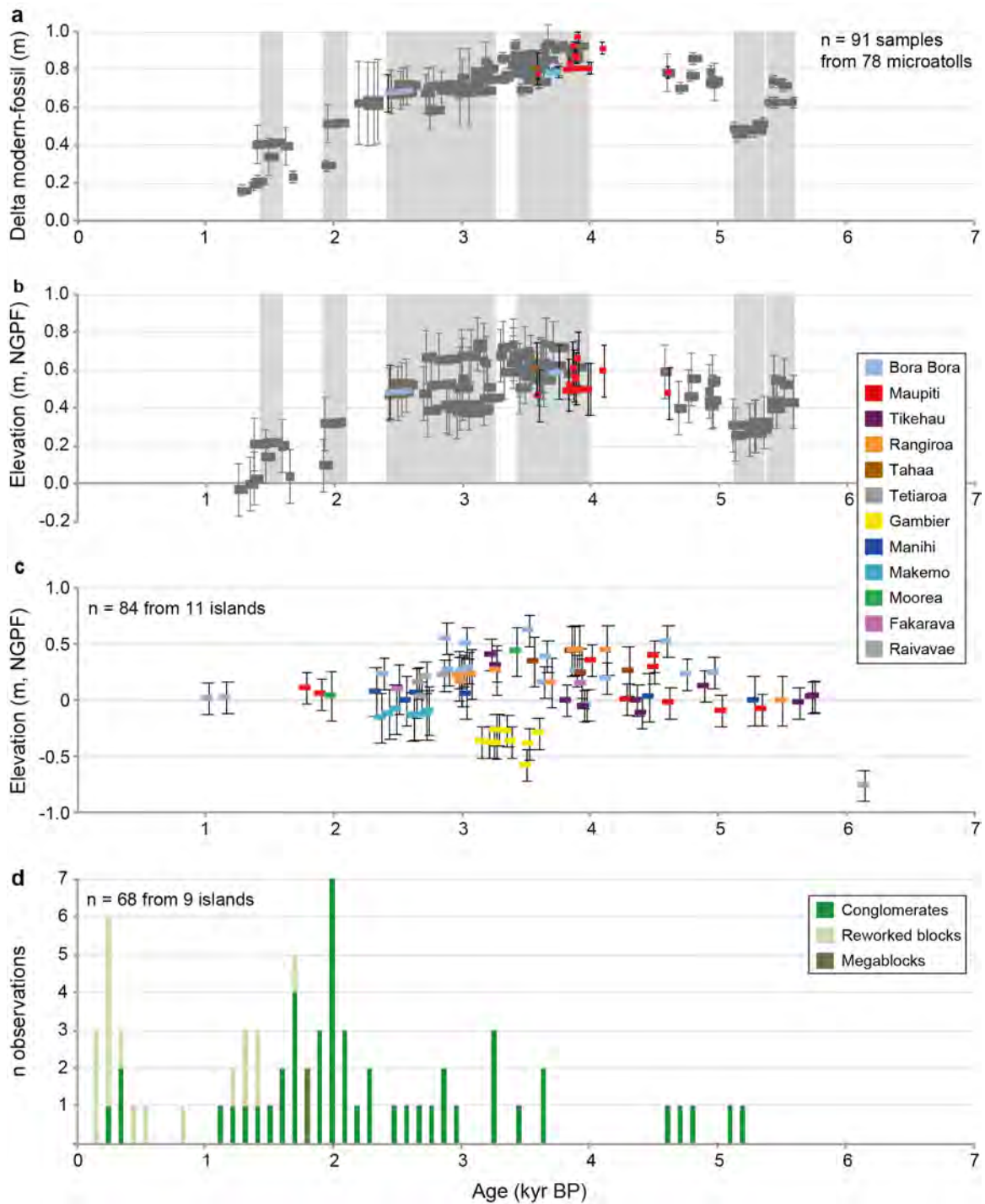


301

302 Fig. 6. Morphological units of a Bora Bora study site (Motu Mute). Hol mic: Holocene
303 microatolls, Mod mic: modern microatolls, Hol rf: Holocene reef flat, Im rf: inner modern
304 reef flat, Om rf: outer modern reef flat, Cgm: conglomerates, Br: beachrock, Rc: reef crest.

305

306 The mid-late Holocene sequence encompasses the last 6,000 years (Fig. 7). It forms
307 distinctive elevated terraces that are comprised of coral microatoll terraces (Fig. 1d), which
308 generally rest on, or are connected laterally to, Holocene reef flat units. Coral microatoll
309 terraces and reef flat units are unevenly covered by thick accumulations of conglomerates
310 composed of reworked coral colonies (e.g., Matuura/Tikehau, northern part of Rangiroa,
311 Makemo), and interpreted as storm deposits (Figs. 4-6). The palaeobiological composition
312 and facies distribution of mid-late Holocene reef units are similar to their modern
313 counterparts.



314

315

316

317

318

319

Fig. 7. Mid-late Holocene RSL changes and reef development. (a) Age vs elevation plot of dated microatolls. Calculated elevations are based on the height difference between living microatolls and their fossil counterparts ('Delta modern-fossil'). The grey shaded areas indicate specific time windows characterized by century-scale stillstands during which large microatolls with a diameter of ≥ 2.5 m developed. Data concerning Tetiaroa were obtained

320 during a parallel study (A.E., unpublished). (b) Age vs elevation plot of dated microatolls.
321 Elevations are based on NGPF measurements (geodetic datum in French Polynesia).
322 (c) Age vs elevation plot of dated *in situ* reef flat facies. Elevations are based on NGPF
323 measurements (geodetic datum in French Polynesia). (d) Age distribution of conglomerates
324 and reef boulders.
325 For (a) and (b), the grey data points are from Hallmann et al. (2018) and the data points in
326 other colours are from this study. Error values for ages and elevations are 2-sigma
327 (Hallmann et al., 2018) in (a), (b) and (c). Elevations have been corrected for subsidence
328 (see Supplementary Table 1).

329

330 4.1.1. *Microatolls and microatoll fields*

331 At our study sites, modern coral microatolls are mostly made by *Porites* (Fig. 1a, b) and, to a
332 lesser extent, merulinids. They are especially abundant on Bora Bora, Maupiti, Tahaa,
333 Tikehau, Manihi and Makemo, and scarce on Tahiti, Fakarava, Rangiroa and Raivavae. On
334 the Society Islands, microatoll fields exclusively occur in the northern part of the islands.
335 Modern coral microatolls were not observed on Raiatea, Moorea, Hao, Tubuai and the
336 Gambier Islands. The diameters of modern coral microatolls range from 0.2 to 1 m (0.5 m on
337 average) and therefore represent a time span of 10 to 50 years based on the average growth
338 rate (12 mm/yr) of modern *Porites* colonies in the study area (Farley et al., work in progress).
339 The largest reported modern *Porites* microatoll displays a diameter of 3 m and is located on
340 Fakarava. The top of modern living microatolls, called the ‘biological level’, occurs at 0.18 m
341 deep in reef flat environments, at 0.23 m in lagoonal areas and at 0.26 m in *hoas* (Hallmann et
342 al., 2018), thus reflecting short-term changes in water level induced by winds and/or swells or
343 local hydrodynamic conditions (Pirazzoli and Montaggioni, 1984; Rougerie, 1995). No
344 moating effect is reported on the studied islands, thus implying that the palaeo-water depth
345 significance of Holocene coral microatolls is well constrained to 0.18 to 0.26 m, depending on

346 the environment. Continuous growth of coral microatolls therefore indicates a sea-level
347 stability during their lifetime, involving variations in sea level smaller than 20 cm.
348 Holocene *Porites* microatolls were reported on seven of the 15 studied islands where they
349 display a specific distribution related to prevailing environmental conditions. They occur from
350 0.03 m deep to 0.65 m high and give ages ranging from 4.96 ± 0.07 to 1.38 ± 0.03 kyr BP on
351 the Society Islands and from 5.59 ± 0.05 to 1.26 ± 0.02 kyr BP on the Tuamotus
352 (Supplementary Table 1), thus encompassing most of the mid-late Holocene time span. Only
353 reworked coral microatolls were observed on Fakarava and Manihi. Like their modern
354 counterparts, Holocene microatolls have not been reported on the Austral and Gambier
355 Islands. The surface covered by Holocene microatoll fields generally represents 1 to 6% of the
356 studied areas; fields of Holocene microatolls were not reported in the northern part of
357 Rangiroa and on Makemo.

358 Individual Holocene coral microatolls display a wide range of diameters, from 0.2 to 6.2 m,
359 and typify sea-level stillstands on decadal to centennial time scales when sea-level variations
360 were smaller than 20 cm over the corals' lifetime. Most microatolls (~75%, n = 149) average
361 0.6 to 1.7 m in diameter and therefore represent a time span of 25 to 70 years. Significantly
362 larger microatolls, displaying diameters ranging from 2.5 to 6.2 m, occur on Bora Bora,
363 Maupiti and Tikehau, indicating longer sea-level stillstands (i.e., up to 250 years) during six
364 specific time windows between 5.59 ± 0.05 and 1.38 ± 0.03 kyr BP, i.e. during most of the
365 mid-late Holocene sea-level history (Fig. 7a, b).

366 Coral microatolls usually form compact fields, especially on Tikehau, Bora Bora and Maupiti.
367 In contrast, when the assemblages are looser, the spaces between the coral microatolls are
368 filled by *in situ* and reworked coral colonies, including branching *Acropora* and *Pocillopora*
369 exhibiting a lateral growth pattern, massive merulinids and *Porites*, lamellar and
370 pseudocolumnar *Porites* and solitary *Fungia*; bivalves (mainly *Tridacna*) are common.

371

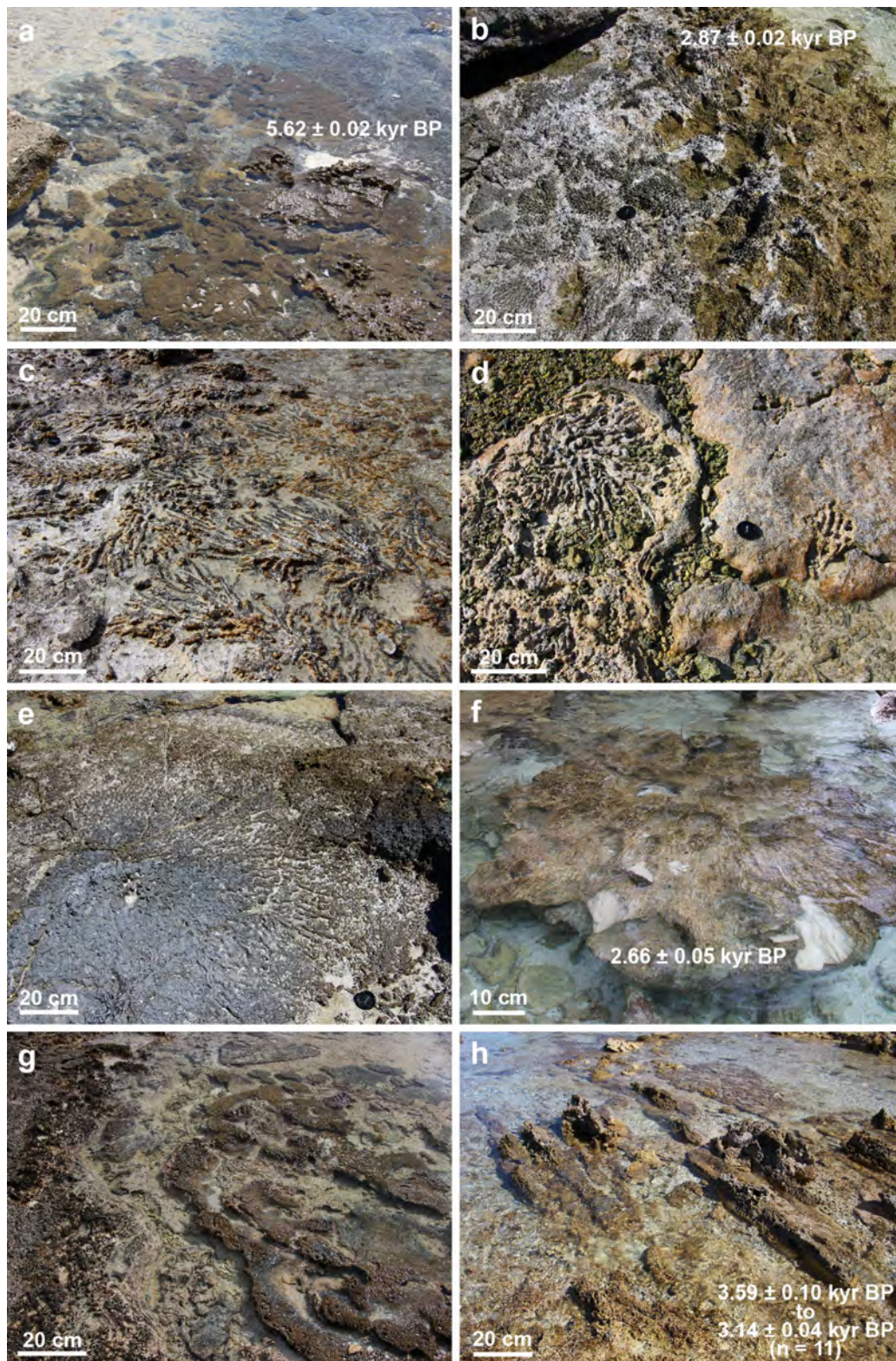
372 4.1.2. Reef flat units

373 Holocene reef flat units generally occur seawards of coral microatoll fields (Figs. 5, 6) and
374 commonly exhibit a gentle seaward slope. They mainly occur close to modern mean sea level,
375 from 0.4 m high to 0.2 m deep, where they form the substrate of the modern shoreline and
376 display a typical brownish colour (Fig. 8a). They have been observed on ten studied islands
377 where they encompass different time windows covering most of the mid-late Holocene, from
378 5.76 ± 0.17 to 3.41 ± 0.07 kyr BP on the Society Islands and from 5.75 ± 0.03 to 2.31 ± 0.02
379 kyr BP on the Tuamotus (Figs. 7, 9; Supplementary Table 1). The oldest dated *in situ* coral
380 sample has an age of 6.13 ± 0.07 kyr BP and corresponds to a flat coral colony included in
381 reef flat units occurring at 1 m deep on Raivavae (Ruahota Rahi). Reef flat units cover
382 surfaces that currently represent 9 to 46% of the studied areas, with an average of 25%;
383 however, their maximum extension during the mid-late Holocene is estimated to have been
384 four to seven times larger, in relation to the higher sea-level stand.

385 Their composition is similar to that of their modern counterparts and consist of *in situ* and
386 reworked coral colonies of robust branching *Acropora* and *Pocillopora* (Fig. 8b-e), massive
387 *Porites* and foliaceous merulinids, while *Millepora* and solitary *Fungia* are clearly
388 subordinate. Branching coral colonies generally display a lateral growth pattern, which
389 indicates that their growth was influenced or even limited by sea surface and/or tidal currents.

390 Dense assemblages of flattened branching or foliaceous coral colonies locally end up with the
391 formation of a compact pavement. The outer margins of patches of branching colonies are
392 commonly overgrown by lamellar *Porites* colonies and then coated by thick coralline algal
393 crusts. Flat *Porites* colonies averaging 0.7 m and up to 6.5 m in diameter (e.g., on Maupiti)
394 and, to a lesser extent, meandroid corals with an elongated to circular shape (Fig. 8f) are
395 common components of Holocene reef flat units. These colonies have developed under the
396 influence of the tidal regime and may correspond to an early microatoll development stage
397 (see Hopley et al., 2007), generally at a few tens of centimetres to 1 m below the sea surface,

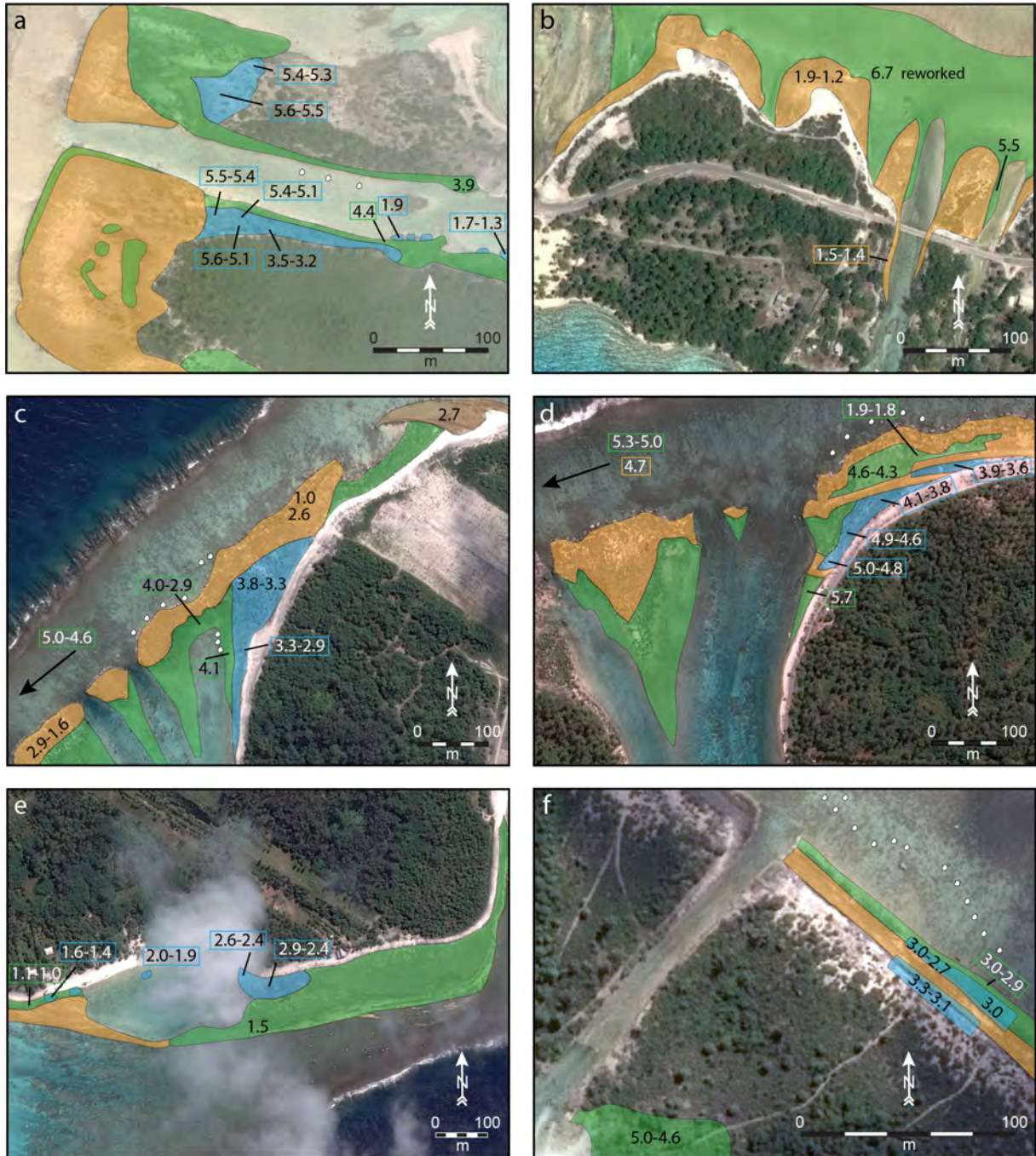
398 and up to 1.5 m deep in areas typified by a greater tidal range (e.g., Gambier Islands). They
399 can be therefore considered as lower limit indicators and their dating therefore helps to further
400 constrain sea-level changes and reef responses to those changes. The common elongated
401 morphology of these coral colonies, the occurrence of ridges that are perpendicular to the
402 shore and the presence of thick crusts of *Porolithon* gr. *onkodes* (Fig. 8g, h) reflect their
403 growth in an environment dominated by high-energy conditions (Camoin et al., 2012).
404 Subcolumnar *Porites* colonies may occur between large flat *Porites* colonies.
405 The upper surface of reef flat units displays abundant algal crusts and mollusks (mostly
406 *Tridacna*); it is commonly irregular and exhibits bioerosion features as well as cavities and
407 conduits that are partly filled by pieces of microatolls reworked from the overlying unit,
408 indicating that they correspond to post-depositional erosional processes.



409

410 Fig. 8. Holocene reef flat units. (a) Reef flat with massive colonies (Tikehau). (b) and (c)
 411 Reef flat with branching *Acropora* (Bora Bora and Maupiti). (d) Reef flat with branching
 412 and massive corals thickly encrusted by coralline algae (Maupiti and Bora Bora). (e) Reef
 413 flat with large branching colonies displaying a lateral growth pattern (Tikehau). (f) Flat,

414 meandroid coral colony (Raivavae). (g) Reef flat with branching and massive corals
 415 encrusted by coralline algae (Maupiti and Bora Bora). (h) Reef flat with elongated *Porites*
 416 colonies (Gambier Islands).



417
 418 Fig. 9. Ages and distribution of morphological units. (a) Motu Matuura, Tikehau. (b)
 419 Taamoi, Rangiroa. (c) Motu Mute, Bora Bora. (d) Motu Tuanai, Maupiti. (e) Motu Piti Aau,
 420 Bora Bora. (f) Motu Ome, Bora Bora. Blue: Holocene microatolls, green: Holocene reef flat,
 421 orange: conglomerates. The white circles indicate the position of major living microatolls.

422 The exact position of some samples cannot be shown on this map section and is indicated by
423 a black arrow. Their position is shifted by a few hundreds of metres in arrow direction.

424

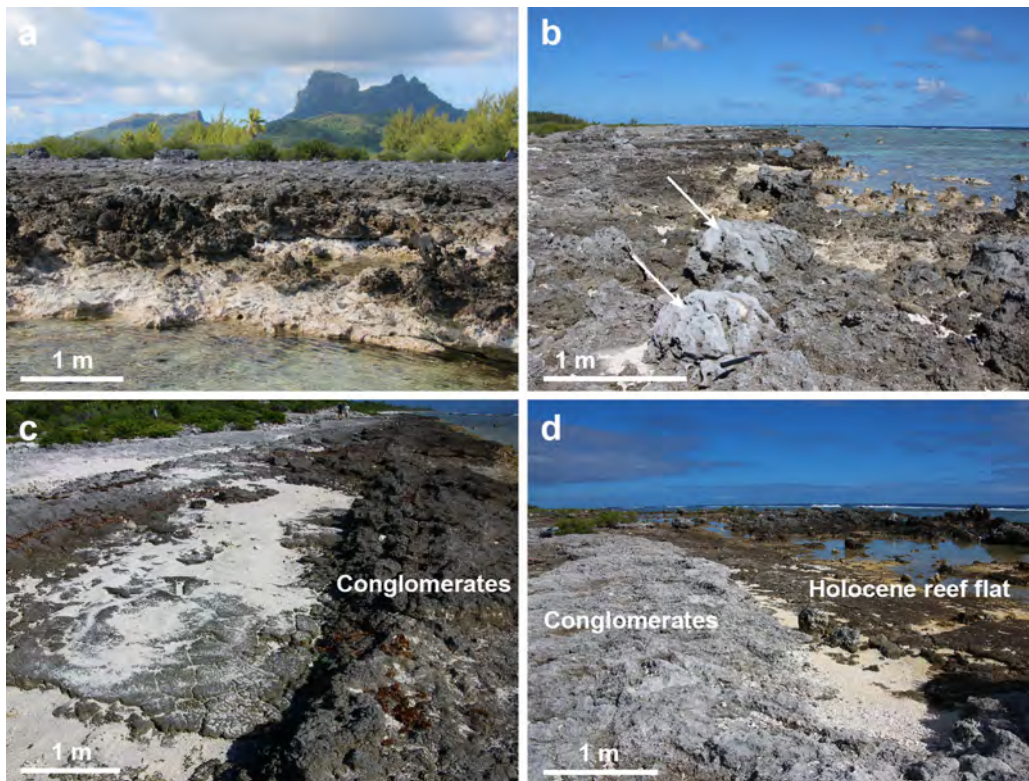
425 *4.1.3. Conglomerates and reworked reef blocks*

426 On all studied islands, Holocene coral microatoll terraces and reef flat units are unevenly
427 covered by accumulations of poorly-sorted conglomerates of variable thickness up to 1.5 m
428 thick (Figs. 4-6; Fig. 10a-d) and covering 4 to 26% of studied areas, with an average of 15%.

429 These conglomerate units are usually comprised of successive beds displaying sedimentary
430 slopes dipping seawards; they thicken in the direction of the open ocean and pinch out in the
431 direction of the lagoon. They form significant reliefs along the modern coastline, generally
432 parallel to it, and may form scattered islets in the lagoon. They often plaster the morphology
433 of underlying units, especially microatoll fields (Fig. 10c), and/or pinch out against antecedent
434 topography formed by *feos* on Tikehau and Rangiroa. Their upper surface commonly forms
435 an overall flat, near-horizontal platform suggesting the occurrence of subsequent abrasion
436 processes (Fig. 10b).

437 Conglomerates are mostly composed of reworked, disoriented, sometimes eroded and
438 cemented coral colonies and boulders, associated to fragments of corals, mollusks (mostly
439 *Tridacna*, oysters and gastropods) and echinoids; thick coralline algal crusts around coral
440 colonies as well as algal bushes are locally abundant, especially at the top of conglomerate
441 pavements. Coral colonies are usually up to 40-50 cm in size and include especially robust
442 branching *Acropora* and *Pocillopora*, tabular *Acropora*, lamellar and massive *Porites* and
443 merulinids, as well as fewer lamellar and meandroid corals and solitary *Fungia*. Larger
444 scattered dome-shaped colonies of *Porites* (Fig. 10b) and merulinids of up to 1.5 m occur at
445 the top of conglomerate platforms on all studied islands. Rapid grain size variations occur in
446 the matrix of conglomerates and irregular alternations of big fragments, gravels and coarse

447 sand deposits are observed locally; the matrix is commonly composed of *Halimeda*-rich
448 gravels and sands.



449
450 Fig. 10. Conglomerates. (a) Conglomerate platform with an elevation of about 1 m above
451 mean sea level (Bora Bora). (b) Conglomerate platform with reworked, dome-shaped
452 *Porites* colonies (arrows; Bora Bora). (c) Large flat microatoll surrounded by conglomerates
453 (Bora Bora). (d) Holocene reef flat partly covered by conglomerates (Maupiti).

454
455 Sampling of conglomerate units were conducted both at their surface and along vertical
456 sections to avoid sampling bias as much as possible; it is therefore considered as
457 representative of the composition of these units. These units are interpreted to correspond to
458 storm deposits and corals dated from within these units cover a wide range of ages from 5.18
459 ± 0.04 to 0.06 ± 0.01 kyr BP ($n = 48$; Supplementary Table 1). Their occurrence peaks in four
460 distinctive time periods of variable importance: 5.2-4.6, 3.6-3.2, 2.9-1.0 and 0.2-0.1 kyr BP
461 (Fig. 7d); however, their maximum occurrence is reported between 2.2 and 1.5 kyr BP.
462 Sustained storm activity during these periods is in good agreement with data obtained on

463 Tahaa, where two prominent intervals of increased storm-derived coarse-grained deposition
464 were reported: 5.0-3.8 kyr BP and 2.9-0.5 kyr BP (Toomey et al., 2013). On most islands,
465 conglomerate units are usually overlain by recent beachrock deposits rich in coral fragments
466 and *Tridacna* shells.

467 On all studied islands, loose reef boulders of several metres in size rest on various parts of the
468 modern reef system, especially on the reef flat and in lagoonal areas. They are interpreted as
469 having been plucked from the adjacent reef and transported by storm waves. Ages obtained
470 from storm boulders range from 1.74 ± 0.01 to 0.04 ± 0.02 kyr BP, with a maximum
471 occurrence between 1.7 and 1.1 kyr BP, and 0.4 and 0.04 kyr BP; they are especially abundant
472 on Fakarava (Fareana) where the largest blocks have been dated at 1.7 kyr BP.

473

474 *4.2. The evolution of the mid-late Holocene reef complex through time*

475 Mid-late Holocene RSL changes encompassing the last 6,000 years on a century time scale
476 are reconstructed based on high-precision GPS positioning and U/Th dating of 78 *in situ* coral
477 microatolls from five islands (Hallmann et al., 2018) and 13 samples from six additional
478 microatolls in the frame of the current study (Figs. 7, 11). The elevations of Holocene
479 microatolls have been directly compared to those of their living counterparts growing in the
480 same depositional environment to track relative changes of the MLWS level throughout the
481 mid-late Holocene (Fig. 7a). It has been assumed that the relationship between microatolls
482 and the tidal cycle has remained the same over the last 6,000 years (Hallmann et al., 2018).
483 Moreover, GPS measurements of microatoll elevations have been referenced to local tidal
484 parameters defined by the NGPF (Fig. 7b). In addition, the dating of 132 coral samples from
485 mid-late Holocene reef flat units and conglomerates and their vertical and lateral relationships
486 with microatoll fields help to further constrain relative sea-level changes and to reconstruct
487 successive stages of reef development (Fig. 7c, d). The curve based on dated reef flat units
488 follows the reconstructed sea-level curve based on microatolls, but lies generally 0.3 to 0.4 m

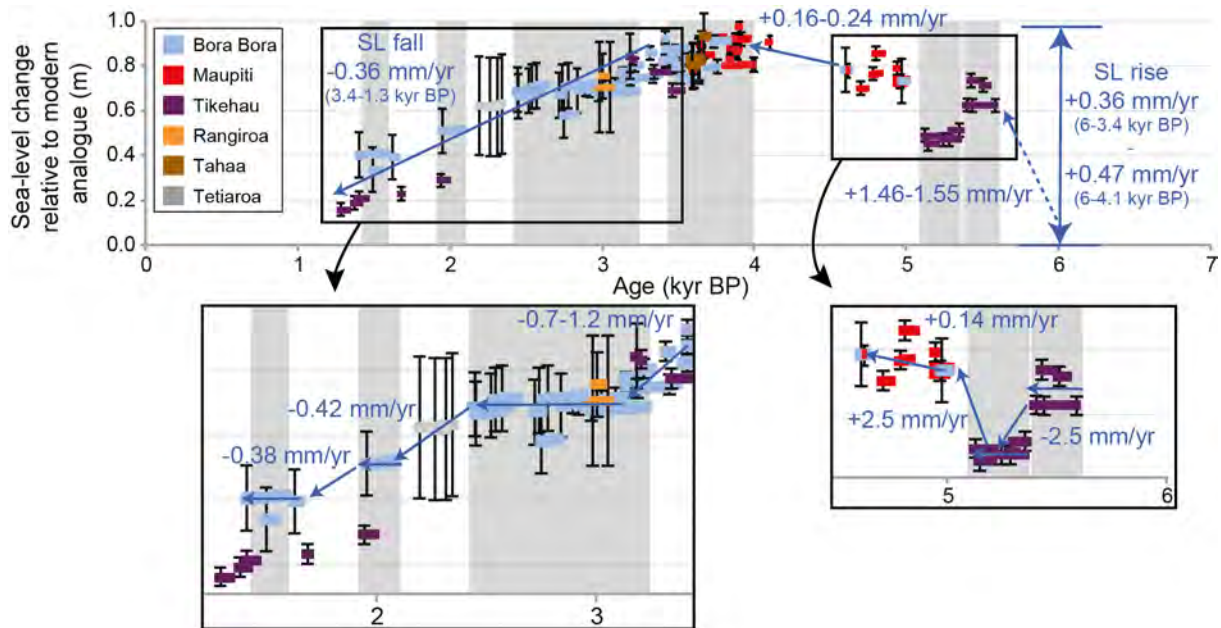
489 below it on average, thus reflecting the water depth of their depositional environment (Fig.
490 7b).

491 The reconstructed sea-level curve documents a short-lived, ~700-year, sea-level highstand of
492 less than a metre between 4.10 and 3.40 kyr BP, following an overall sea-level rise from 6.0
493 to 4.10 kyr BP and preceding a fall in sea level between 3.40 and 1.26 kyr BP (Figs. 7, 11).

494 As a consequence of these low-amplitude sea-level variations, successive generations of coral
495 microatolls and associated reef deposits are usually mixed and the reconstruction of reef
496 development relies both on accurate U-series dating and relevant GPS positioning, and on the
497 relationships between different reef facies in successive time windows. Three islands
498 document significant time windows of the sea-level history:

- 499 - Tikehau, where a sea-level fall is recorded between 5.59 and 5.12 kyr BP and during
500 the 3.51-3.19 and 1.96-1.26 kyr BP time windows;
- 501 - Maupiti, where a sea-level rise is documented between 4.99 and 4.61 kyr BP and the
502 sea-level highstand between 4.10 and 3.60 kyr BP;
- 503 - Bora Bora, where the sea-level highstand is recorded between 3.81 and 3.40 kyr BP,
504 followed by a fall in sea level between 3.40 and 1.38 kyr BP.

505 The other islands have provided information on shorter time windows, which complemented
506 the data from the three main islands, providing eventually the accurate reconstruction of the
507 mid-late Holocene sea-level history. The high-resolution reconstruction of sea-level changes
508 provides the necessary frame to analyze their impact on reef geometry, composition and
509 evolution over the last 6,000 years, as well as the respective role played by variations in
510 accommodation space, antecedent topography and environmental changes.



511

512 Fig. 11. Rates of mid-late Holocene sea-level change. These rates have been calculated
 513 based on the age and elevation differences between two successive coral microatoll samples
 514 with reference to the elevation of modern microatolls. Error values for ages and elevations
 515 are 2-sigma (see Hallmann et al., 2018). The grey shaded areas indicate specific time
 516 windows characterized by century-scale stillstands during which large microatolls with a
 517 diameter of ≥ 2.5 m developed. Microatoll elevations have been corrected for subsidence
 518 (see Supplementary Table 1).

519

520 *4.2.1. Sea-level rise (6.0 - 4.10 kyr BP; Figs. 7, 11)*

521 The rate of sea-level rise from 6.0 kyr BP to the start of the highstand at 4.1 kyr BP averages
 522 0.36 to 0.47 mm/yr. Microatoll fields on Tikehau (Matuura) occur at two distinctive present
 523 elevations: 0.4-0.5 and 0.3 m. They form terraces that are gently dipping towards the modern
 524 *hoa* and the lower terrace pinches out against the morphology of the upper terrace. They yield
 525 ages ranging from 5.59 ± 0.05 to 5.41 ± 0.08 and 5.37 ± 0.05 to 5.12 ± 0.04 kyr BP,
 526 respectively, thus indicating MLWS levels of 0.6-0.7 m and 0.5 m above the present position
 527 during these time intervals, respectively. These two successive generations of microatolls
 528 therefore document a sea-level rise averaging 1.46 to 1.55 mm/yr between 6.0 and 5.6 kyr BP,

529 followed by a slight sea-level drop of 0.2-0.3 m in amplitude. The relevant microatoll fields
530 are primarily comprised of microatolls larger than 1.6 m in diameter, thus indicating that they
531 developed during sea-level still stands longer than 70 years. These large microatolls have
532 been systematically sampled both at their center and on their outer rim. The largest
533 microatolls, up to 5 m in diameter, belong to the oldest generation. The rate of the sea-level
534 fall that is evidenced between the development of the two microatoll fields is of 2.5 mm/yr
535 (Fig. 11). Coeval reworked microatolls, 0.3 to 0.6 m in diameter, with ages ranging from 5.69
536 ± 0.06 to 5.48 ± 0.09 kyr BP have been observed elsewhere (Matiti, Tikehau). The microatoll
537 fields are associated laterally to reef flat units that occur a few tens of centimetres lower. The
538 vertical succession involving reef flat units overlain by the second generation of microatolls is
539 related to a sea-level drop between 5.43 ± 0.04 and 5.37 ± 0.05 kyr BP. Reef flat units are
540 mostly comprised of *in situ* coral colonies, including large flat *Porites* and merulinids up to a
541 few metres in diameter, branching *Acropora* and *Pocillopora* with a distinctive lateral growth
542 pattern, and lamellar *Porites* that occur at the edge of large flat *Porites* and around coral
543 patches (Fig. 8a); reworked massive merulinids are clearly subordinate.

544 Very slow rates of sea-level rise (0.16-0.24 mm/yr) characterize the end of the 4.6-4.1 kyr BP
545 period when microatoll fields display extensive development. These fields are comprised of
546 coalescing patches of several microatolls ranging from 0.5 to 0.8 m in diameter that are coated
547 by lamellar coral colonies and thick crusts of coralline algae. The depressions between
548 microatolls display a variety of coral colonies including subcolumnar and lamellar *Porites*,
549 branching *Pocillopora* and *Acropora* often characterized by lateral growth pattern, and
550 flattened merulinids; the occurrence of abundant and thick crusts of coralline algae indicates
551 the prevalence of high-energy conditions. These microatoll fields crop out at present
552 elevations of 0.4-0.6 m on Maupiti (Tuanai) and Bora Bora (Ome), indicating that the MLWS
553 level was located at 0.7 to 0.8 m above its present level between 5.0 and 4.6 kyr BP. On
554 Maupiti (Tuanai), these microatolls overlie reef flat units dated at 5.7 kyr BP (Fig. 9). A sea-

555 level rise of 0.2 to 0.3 m at a rate of 2.5 mm/yr is therefore evidenced between 5.12 and 4.99
556 kyr BP (Fig. 11). Reworked microatolls, including large ones of up to 2.6 m in diameter, are
557 reported on Tikehau (Matiti) and yield ages ranging from 5.69 ± 0.06 to 4.75 ± 0.07 kyr BP.
558 The microatoll fields that characterize a sea-level rise between 5.6 and 4.6 kyr BP usually
559 grade laterally to reef flat units that form very flat areas dipping gently seawards at lower
560 elevations than microatoll fields. On Tikehau (Tuherahera), *in situ* flat colonies of *Porites* that
561 are larger than 1 m in diameter, are observed at present mean sea level and yield ages ranging
562 from 5.75 ± 0.03 to 5.62 ± 0.02 kyr BP. Reef flat units include large flat and subcolumnar
563 colonies of *Porites* associated with foliaceous colonies of merulinids characterized by a lateral
564 growth pattern and, to a lesser extent, branching colonies of *Pocillopora* and *Acropora*. High-
565 energy conditions are typified by the occurrence of thick coralline algal crusts, which
566 delineate the various patches composing the fossil reef flat. Cavities, conduits and channels
567 are common in these units and suggest mechanical abrasion and/or dissolution processes.
568 Similar and coeval reef flat units are observed on Bora Bora (Mute, Ome, Iti and Haapitirahi),
569 Rangiroa (Taamoi) and Manihi (Arianohu); reef flat units dominated by robust branching
570 *Pocillopora* and thick coralline algal crusts occur at a current elevation of 0.1-0.2 m on
571 Maupiti (Tuanai) and are dated at 5.76 ± 0.17 and 5.74 ± 0.10 kyr BP. On Tikehau (Matiti),
572 storm deposits comprised of conglomerate units are dated between 5.18 and 5.12 kyr BP and
573 between 4.79 and 4.61 kyr BP, and were therefore deposited during a rise in sea level.

574

575 4.2.2. Sea-level highstand (4.10 - 3.40 kyr BP; Figs. 7, 11)

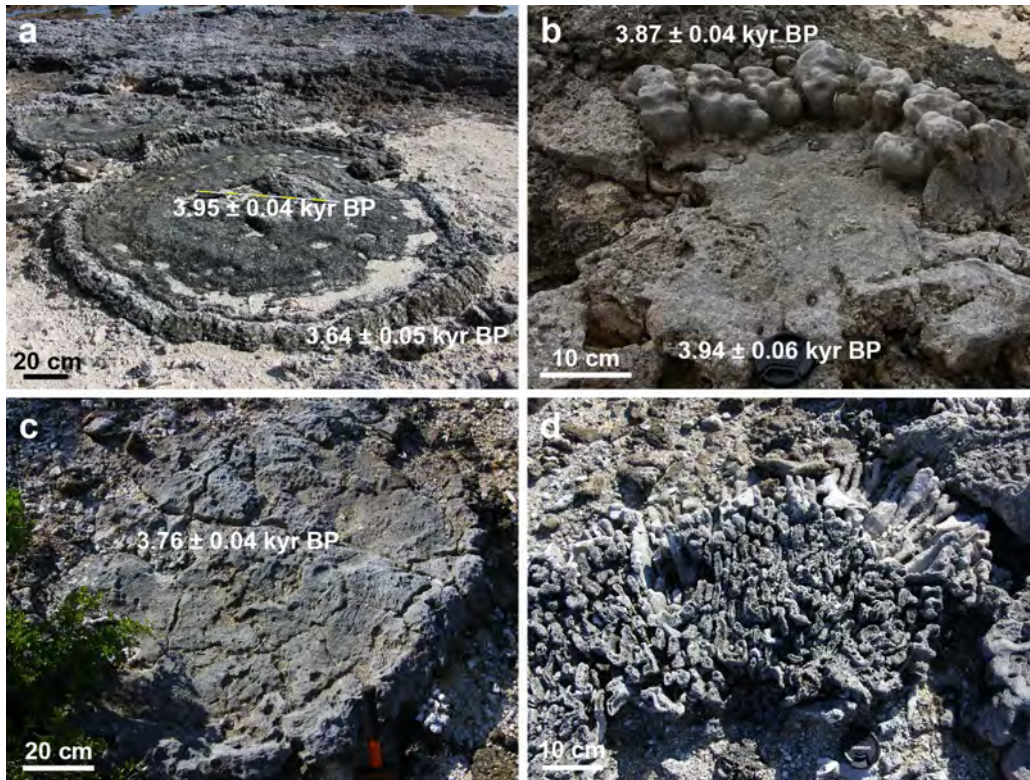
576 A sea-level highstand involving a MLWS level of up to 0.97 m above its present position is
577 inferred between 4.10 and 3.40 kyr BP; the highest elevation has been recorded on Maupiti
578 and corresponds to an age of 3.91 ± 0.03 kyr BP. Our sea-level curve differs markedly from
579 previous reconstructions, which include either a higher amplitude, estimated at a minimum of
580 +1.5 m (Rashid et al., 2014), and/or a much longer sea-level highstand in the 5.0-1.5 kyr BP

581 (Pirazzoli and Montaggioni, 1988) and 5.4-2.0 kyr BP (Rashid et al., 2014) time windows.
582 More generally, most of our microatoll data plot below these former sea-level reconstructions.
583 We assume that these discrepancies may result from inaccurate measurements of elevations
584 and/or from the dating of coral colonies reworked in storm deposits that commonly overlie the
585 microatoll fields.

586 The precise start of the sea-level highstand could not be determined, as no microatoll has been
587 recorded in the 4.6-4.1 kyr BP time interval; thus, the rates of sea-level rise must be
588 considered as minimum values. The lack of microatoll development may result from
589 temporary and/or local changes in environmental conditions, or to a sampling bias despite the
590 thorough exploration of the studied islands. A rapid and short-lived sea-level fall after 4.6 kyr
591 BP, as suggested by other records (Lewis et al., 2008, 2013), cannot be discarded. However,
592 the reef flat units covering the 5 to 4 kyr BP time window do not display any change in their
593 depth distribution, thus arguing against such an interpretation. Large flat colonies of *Porites*
594 and merulinids are observed in reef flat units on Maupiti (Tuanai, Tiapaa) and Rangiroa (Teu)
595 at present elevations of 0.15 to 0.25 m and 0.45 m, respectively, i.e. ~1 m above their modern
596 counterparts. They give ages ranging from 4.48 ± 0.03 to 4.0 ± 0.05 kyr BP on Maupiti and
597 from 4.13 ± 0.03 to 3.87 ± 0.02 on Rangiroa. On Tahaa and Tikehau (Tuherahera, Matiti),
598 corals forming reef flat units occur at present sea level and give ages ranging from 4.29 ± 0.04
599 to 3.55 ± 0.05 and from 4.36 ± 0.01 to 3.80 ± 0.02 kyr BP, respectively.

600 The sea-level highstand is typified by the widespread development of microatoll fields (Figs.
601 1d, 4, 5) that are especially well exposed on Maupiti, Tahaa and Bora Bora (Mute) where they
602 yield ages ranging from 4.10 ± 0.04 to 3.40 ± 0.05 kyr BP. The diameter of the microatolls
603 ranges generally from 0.4 to 1.2 m in diameter, but some individuals are much larger,
604 especially in the 4.0-3.8 kyr BP time window. The largest coral microatoll exhibits a diameter
605 of 2.75 m, equivalent to about 115 years of continuous coral growth; this has been confirmed
606 by direct dating of the central part and the edge of the microatoll colony, which yield ages of

607 3.95 ± 0.04 and 3.84 ± 0.03 kyr BP, respectively. The upper surface of the microatolls is
608 generally flat, but the elevated outer margin of some individuals indicates a slight sea-level
609 rise during their late development, as found on Maupiti (Tuanai) during the 4.1-3.8 kyr BP
610 time window (Fig. 12a-c). This demonstrates that minor sea-level variations have occurred
611 during the sea-level highstand. In the same area, the start of sea-level fall at 3.6 kyr BP is
612 documented by the development of the outer margin of microatolls at a lower elevation than
613 their central part. Branching *Acropora* and *Pocillopora* and pseudocolumnar *Porites* colonies
614 occur between microatolls (Fig. 12d). Microatoll fields overlay reef flat units that were
615 deposited during the former sea-level rise and which form the basement of the current
616 shoreline; on Maupiti (Tuanai), these reef flat units are dated between 4.62 ± 0.05 and $4.29 \pm$
617 0.05 kyr BP. Reef flat units usually occur 0.3 to 0.4 m below coeval microatoll fields, and are
618 slightly inclined seawards. They exhibit a typical brownish colour, a rather compact structure
619 and a very flat topography. On Bora Bora (Mute), reef flat units occur at modern mean sea
620 level and give ages ranging from 4.1 and 2.9 kyr BP (Fig. 9c). Reef flat units are mostly
621 comprised of a dense pavement of large flat colonies of *Porites*, ranging from 1 to 6.5 m in
622 diameter, with a slightly irregular upper surface displaying abundant bioerosion. The largest
623 flat colonies of *Porites* are observed at an elevation of 0.2 m on Bora Bora (Mute) and yield
624 ages ranging from 3.8 to 3.6 kyr BP. Branching colonies of *Acropora* and *Pocillopora* are
625 commonly associated and display a conspicuous lateral growth pattern, indicating that their
626 vertical development was constrained by the water surface and/or tidal currents.



627

628

629

630

631

632

633

634

635

636

637

638

639

640

641

642

Fig. 12. Mid-late Holocene sea-level highstand. (a) *Porites* microatoll with a higher margin indicating a sea-level rise during its growth, and ridges on the surface related to low-amplitude, high-frequency sea-level changes over ca. 140 years (Maupiti). (b) *Porites* microatoll exhibiting overgrowth on its margin reflecting a sea-level rise of about 6 cm (Maupiti). (c) *Porites* microatoll with visible annual growth lines on its surface (Bora Bora). (d) *In situ Pocillopora* branching colony growing between *Porites* microatolls (Bora Bora).

4.2.3. Sea-level fall (3.40 – 1.26 kyr BP; Figs. 7, 11)

The distribution and the dating of microatoll fields from Bora Bora, Tikehau and Rangiroa, document a fall in MLWS level from 0.93 m at 3.40 kyr BP to about 0.16 m at 1.26 kyr BP above its present position, at an average rate of 0.36 mm/yr (Fig. 11). This rate is consistent with data reported from nearby archipelagos like the Cook Islands (Goodwin and Harvey, 2008) and is typical for mid-ocean regions of the South Tropical Pacific during mid-late Holocene (Mitrovica and Milne, 2002). The youngest *in situ* coral microatoll is reported on Tikehau (Matuura) and yields an age of 1.26 ± 0.02 kyr BP; younger reworked microatolls

643 dated 1.15 ± 0.02 and 1.16 ± 0.02 kyr BP have been recorded on Fakarava (Vahapiapia). Our
644 results are therefore in clear contradiction with the occurrence of a short-lived sea-level peak
645 of 1 m in amplitude between 2.0 and 1.5 kyr BP (Pirazzoli and Montaggioni, 1988).

646 The occurrence of large microatolls of more than 2.5 m in diameter in three specific time
647 windows, 3.2-2.4, 2.1-1.9 and 1.6-1.4 kyr BP, characterizes relative sea-level stillstands
648 longer than 100 years (Fig. 11). This indicates that sea level did not fall at a continuous rate,
649 but was characterized by significant variability, involving extended periods of relative sea-
650 level stability.

651 The 3.4-3.1 kyr BP time span is characterized by rates of sea-level fall ranging from 0.7 to 1.2
652 mm/yr (Fig. 11). It is documented by microatoll fields that occur at present elevations of 0.4
653 to 0.7 m on Bora Bora (Mute) and Tikehau (Matuura), respectively, thus characterizing a
654 MLWS level at about 0.5 to 0.8 m above its present position and slightly lower than during
655 the former sea-level highstand. On Bora Bora, the microatoll fields rest on previous reef flat
656 units, indicating a lowering of the sea level. In contrast, on Tikehau (Matuura), they overlay
657 microatoll fields developed during the 5.6-5.1 kyr BP time span and reef flat units dated at
658 4.89 ± 0.05 kyr BP. This indicates that there was no coral growth at that site for at least 1,500
659 years (i.e. between 4.89 and 3.4 kyr BP), especially during the whole duration of the sea-level
660 highstand. This may be due to unfavorable high-energy conditions during this period, as this
661 area is located in the most exposed side of the atoll. Microatoll fields on Bora Bora are
662 comprised of closely packed colonies generally ranging in diameters from 0.2 to 2 m in
663 diameter, the larger ones yielding ages of 3.4 kyr BP. Some colonies display an irregular
664 topography typified by concentric ridges and indicating low amplitude sea-level variations at
665 the start of the sea-level fall. The occurrence of a peripheral ridge at a lower elevation than the
666 core of the colony indicates a sea-level fall during the development of the microatoll, as found
667 on Bora Bora (Mute) for a microatoll dated at 3.40 ± 0.05 kyr BP.

668 The 3.1-2.7 kyr BP time span is typified by a very stable sea-level position allowing the
669 widespread development of compact microatoll fields at elevations of 0.7 m above present
670 MLWS on two islands: Bora Bora (Mute, Ome) and Rangiroa (Teu, Vaihoha) where they
671 cover former reef flat units. *Porites* microatolls display diameters larger than 0.7 m,
672 commonly larger than 2 m and up to 5 m, thus typifying stillstands lasting for up to 200 years
673 long. In contrast, merulinid microatolls generally display diameters less than a metre. The
674 development of thick coralline algal crusts at the edge of coral microatolls indicates the
675 prevalence of high-energy conditions.

676 The 2.70-1.26 kyr BP time window is especially well documented in the southern part of Bora
677 Bora (Piti Aau) where microatoll fields are distributed at elevations ranging from about 0.7 to
678 0.4 m above present MLWS level, with ages of 2.76-2.43 and 1.93-1.38 kyr BP. This
679 descending succession of microatolls (Fig. 1g, h) typifies a fall in sea level at rates ranging
680 from 0.38 to 0.42 mm/yr (Fig. 11). A similar succession close to modern sea level is observed
681 on Tikehau (Matuura) and corresponds to the 1.92-1.26 kyr BP time window, thus
682 documenting the last part of the sea-level fall with a MLWS level falling from 0.29 to 0.16 m
683 above its present position. Their development on reef flat units dated at 4.39 ± 0.06 kyr BP
684 that occurs at modern sea level indicates a hiatus coinciding with the sea-level highstand at
685 that particular site; this hiatus could be related to local unfavorable high-energy conditions
686 during this period. Most microatolls characterizing the 2.70-1.26 kyr BP time window
687 coalesce laterally to form compact fields and display large diameters, commonly larger than
688 2.5 m, thus recording extended sea-level stillstands. The overall upper surface of microatolls
689 is flat, but also exhibit a microtopography that reflects high-frequency and low-amplitude
690 (less than 20 cm) sea-level variations during this time window.

691 All generations of microatolls developed during the sea-level fall are associated laterally to
692 reef flat units that are slightly inclined seawards and occur at lower elevations than microatoll
693 fields. Reef flat units that were deposited during this fall in sea level also occur on islands

694 where microatoll fields do not crop out, such as Mangareva (Tepapuri), Manihi (Pomagu),
695 Hao, Makemo (Oehava), Tahaa, Moorea (Fareone, Tiahura) and Fakarava (Fareana,
696 Vahapiapia). They are primarily composed of *in situ* colonies of massive and flat *Porites* and
697 merulinids, branching *Acropora*, and to a lesser extent *Pocillopora*, that are characterized by a
698 lateral growth pattern, and lamellar *Porites* that develop at the margins of clusters of coral
699 colonies and around large flat coral colonies. The upper surface of coral colonies is generally
700 irregular and exhibits abundant bioerosion features. Reworked coral colonies are locally
701 abundant. On Raivavae (Araoo), flat colonies of meandroid corals and merulinids, 0.3 to 1 m
702 in diameter (Fig. 8f), overlay a karstified reef flat bearing *Acropora* colonies to form a
703 compact field at present elevations of 0.10 to 0.15 m; they yield ages ranging from $2.86 \pm$
704 0.03 to 2.65 ± 0.05 kyr BP.

705 Most of the conglomerate units corresponding to storm deposits, which represent a major
706 component of the mid-late Holocene sequence (Figs. 9, 10), were deposited during the
707 duration of the sea-level fall. However, they are especially conspicuous during the 2.2-1.5 kyr
708 BP time span, indicating sustained storm activity during this period. These storm deposits
709 usually cover microatoll fields and reef flat units. However, on Bora Bora (Piti Aau), they are
710 interlayered between generations of microatolls, thus indicating that their deposition was
711 locally coeval to the development of microatolls.

712

713 **5. Discussion**

714 *5.1. Reef and coastal responses to sea-level and associated environmental changes over the* 715 *last 6,000 years*

716 The impact of future sea-level rise on coastal ecosystems is amongst the most pressing
717 scientific and societal issues posed by warming from greenhouse gas forcing. This problem is
718 especially acute for low-lying islands, which will face dramatic issues in the context of future
719 sea-level rise (IPCC, 2018). There is therefore a clear need to investigate coastal and coral

720 reef responses to low-amplitude, high-frequency sea-level changes that are expected to
721 dominate over the coming decades. However, so far, these processes have been scarcely
722 documented in the mid-late Holocene (Hopley, 1982; Hopley et al., 2007; Harris et al., 2015),
723 and nowhere near at the temporal and spatial resolutions that are needed to better predict the
724 future evolution of coastal systems, especially coral reefs. Furthermore, the impact of mid-late
725 Holocene sea-level change and other environmental factors on reef architecture and
726 composition remains poorly resolved (Camoin and Webster, 2015).

727 The mid-late Holocene reef sequence presented in this study provides the opportunity to
728 document at high-resolution the response of coral reefs and coastal systems to sea-level
729 changes over the last 6,000 years, a period that is typified by slow-rate, low-amplitude and
730 high-frequency sea-level changes. The high-resolution reconstruction of reef geometry,
731 composition and evolution during this time window summarizes the adjustments that reef
732 systems have had to make to changes in accommodation space driven by variations in relative
733 sea level (sea-level rise, stillstand and fall). It therefore helps in the understanding of reef
734 dynamic processes that are of global importance. In addition, it has potentially important
735 implications for predicting how modern reefs might respond to a sea-level rise of similar
736 amplitude, 0.5 to 1.5 m, before the end of the current century (Alley et al., 2007; Church et
737 al., 2013; IPCC, 2018). In this study, a special emphasis has been given to understand how
738 reef areas that are at or near sea level, e.g., microatoll fields and reef flat units, have
739 responded in terms of reef development, architecture and composition to changes in
740 accommodation space, which is controlled by changes in relative sea level and antecedent
741 topography.

742 In French Polynesia, drill core data have demonstrated that coral reefs have accreted
743 continuously over the last 16,000 years, mostly through aggradational processes, at growth
744 rates averaging 10 mm/yr (Camoin et al., 2012). Growth rates then decreased sharply
745 throughout the Holocene to about 0.4 mm/yr during the stabilisation of the sea level at its

746 present position at 6 kyr BP (Cabioch et al., 1999; Camoin et al., 1999, 2001; Hallmann et al.,
747 2018) as a consequence of decreasing accommodation space. On Bora Bora, the Holocene
748 fringing reefs started to develop at 8.7 kyr BP, retrograded over a Pleistocene fringing reef
749 until ca. 6 kyr BP, and then prograded towards the lagoon after sea-level had reached its
750 present level (Gischler et al., 2016, 2019).

751 After the stabilisation of sea level at its present position, the new development of reef systems
752 was initiated by the creation of accommodation space due to a glacio-eustatic sea-level rise,
753 most likely sourced from Antarctica, and controlled by the antecedent topography of the
754 islands. The reversal from rise to fall records the time at which the eustatic signal reduced and
755 GIA (syphoning) became dominant, thus controlling regional histories of reef development.

756 The reconstructed sea-level curve is almost continuous over the last 6,000 years (Hallmann et
757 al., 2018). It unravels mid-late Holocene RSL changes in unprecedented detail and has
758 therefore a global significance. Regional differences between the mid-late Holocene sea-level
759 curve defined in French Polynesia and sea-level data obtained in neighbouring islands and
760 continental margins can be resolved through the use of geophysical models to decipher GIA
761 processes (Botella, 2015; Hallmann et al., 2018).

762 The course of RSL is characterized by the occurrence of a single short-lived sea-level
763 highstand of less than one metre between 4.10 and 3.40 kyr BP, which enhanced reef
764 development, followed by a sea-level fall leading to the partial emergence of the mid-late
765 Holocene reef system (Figs 7, 11). Overall, sea-level changes are characterized by slow rates
766 and low amplitudes. All periods of the sea-level history are characterized by significant sea-
767 level stability (stillstands) lasting more than a century and up to 250 years, as demonstrated by
768 the occurrence of large microatolls ranging from 2.5 to 6.2 m in diameter in specific time
769 windows. This defines a stepped pattern for the sea-level rise and fall, involving periods of
770 sea-level stability and periods of slow sea-level variations at rates ranging from a few tens of
771 millimetres per year to up to 2.5 mm/yr (Fig. 11). This last value is similar to the average rise

772 in sea level that has been recorded over the 1950-2010 time span in French Polynesia
773 (Meysignac et al., 2012).

774 The complex microtopography of some large microatolls exhibiting ridges and different
775 generations of overgrowths with heights of up to 20 cm reflects high-frequency, low-
776 amplitude decadal to sub-decadal sea-level variations superimposed on longer term sea-level
777 changes. This sea-level variability may have been driven by climatic oscillations such as
778 ENSO (El Niño-Southern Oscillation) and PDO (Pacific Decadal Oscillation), which induce
779 sea-level highs and lows of such an amplitude compared to normal conditions in the western
780 Tropical Pacific (Becker et al., 2012; Church et al., 2013). However, some of this variability
781 could be due to the 18.6-year tidal cycle (Meltzner et al., 2017).

782 Continuous reef development was maintained throughout the last 6,000 years with no break in
783 reef growth being identified during this time window, with the exception of the site of
784 Matuura on Tikehau due to local environmental conditions during the mid-late Holocene
785 highstand. The only period during for which no microatoll development was recorded
786 concerns the 4.6-4.1 kyr BP time window and may reflect a sampling bias in the studied
787 islands. This contrasts with some other Pacific regions, including the southern Great Barrier
788 Reef (One Tree Reef) where the lack of coral microatolls younger than 2 kyr BP and the turn-
789 off of reef flat carbonate production were interpreted as resulting from a 1.0-1.3 m fall in sea
790 level (Harris et al., 2015).

791 Mid-late Holocene coral assemblages and their modern counterparts display similar overall
792 composition and diversity, in agreement with the analysis of coral communities during the
793 same time window on the Great Barrier Reef (Roche et al., 2011). Since corals are sensitive to
794 subtle ecological changes affecting their environment (e.g., Camoin and Webster, 2015), this
795 suggests that most of the environmental parameters, such as light conditions, turbidity, water
796 energy and nutrient levels, did not significantly change over the last 6,000 years, with the
797 exception of the hydrodynamic regime. Moreover, the persistence of stable depositional

798 environments and facies distribution is demonstrated by the almost continuous development
799 of microatolls, which typify optimal environmental conditions for their growth during this
800 time window. Furthermore, the recurrent sea-level stillstands that punctuated the mid-late
801 Holocene sea-level history may have played a significant role in the widespread development
802 of dense reef frameworks.

803 The facies distribution and the lateral extension of the facies belts were governed by
804 variations in accommodation space, which are mostly controlled by relative sea-level changes
805 and the antecedent topography. A lateral shift of facies belts typifies sea-level changes during
806 the relevant period, involving a transgressive pattern ('retrogradation') during sea-level rise
807 and an oceanward shift during the subsequent sea-level fall. In contrast, there was no change
808 in accommodation space during the sea-level highstand period (4.1 to 3.4 kyr BP) and
809 recurrent periods of sea-level stillstands, which lasted more than a century and up to 250
810 years. During the mid-late Holocene, microatoll fields have migrated accordingly a few tens
811 of metres and up to 200 m, depending on the palaeotopography of the islands. The surface
812 that they cover did not change significantly over the last 6,000 years and represents 1 to 6% of
813 the reef system in the studied areas. However, the development of microatoll fields was not
814 uniform as it was subordinate to specific environmental conditions in localized areas.

815 In contrast to microatoll fields, reef flat units were much more developed during the mid-late
816 Holocene compared to modern environments, with a maximum extension that was estimated
817 to be four to seven times larger compared to their modern counterparts. This extensive
818 development occurred in prevalent high-energy and very shallow-water conditions. The
819 lateral extension of reef flat units during the mid-late Holocene sea-level rise and sea-level
820 highstand has been clearly subordinate to the antecedent topography and their lateral shift
821 usually ranges from 200 to 500 m. Their development has therefore played a prominent role
822 in reef dynamics as they usually form the substrate of microatoll fields during the sea-level
823 highstand, which occurred between 4.1 and 3.4 kyr BP, but also in the subsequent

824 development of modern islands by providing a substrate for subsequent sediment
825 accumulation.

826 The situation described in French Polynesia contrasts with the southern and northern Great
827 Barrier Reef, where a 2.3-kyr hiatus in lateral reef accretion has been documented from 3.9 to
828 1.5 kyr BP, as a consequence of a relative fall in sea level of ~0.5 m from its maximum
829 highstand at approximately 4.0-3.5 kyr BP (Lewis et al., 2013; Dechnik et al., 2017).

830 However, a fall in sea level and subsequent reef turn off at ~3.6 kyr BP is apparently not
831 supported by microatoll data from One Tree Reef (Harris et al., 2015). On the inner Great
832 Barrier Reef, a new phase of reef flat development occurred at approximately 2 kyr BP
833 following a 3.2-kyr hiatus in reef growth (Perry and Smithers, 2011). Greater hydro-isostatic
834 adjustment and subsidence along the Australian continental margin may have provided greater
835 vertical accommodation for mid-outer reefs of the central Great Barrier Reef where no hiatus
836 in reef flat development was reported (Dechnik et al., 2017).

837 On the Keppel Islands, Leonard et al. (2016, 2018) identified a hiatus in reef flat growth
838 between 4.6 and 2.8 kyr BP, with a possible earlier fall in relative sea level at ~5.5-5.3 kyr
839 BP. However, the timing and course of the relative sea-level fall after the mid-Holocene
840 highstand on the Great Barrier Reef has been interpreted in different ways, through a
841 smoothly falling sea level to present (Chappell, 1983), an abrupt sea-level fall after ~2 kyr BP
842 (Sloss et al., 2007) or 1.2 kyr BP (Lewis et al., 2015), or an oscillating sea level involving
843 metre-scale fluctuations (Lewis et al., 2008; Leonard et al., 2016, 2018).

844 Conglomerate accumulations and pavements comprise the third component of the mid-late
845 Holocene reef sequence in French Polynesia, where they represent a prominent morphological
846 feature, which is up to 1.5 m-thick and covers surfaces ranging from 4 to 26% (average: 15%)
847 of the studied areas. This suggests that these units may have played a prominent role in the
848 recent development of the islands, especially as they accumulated mostly during the late
849 Holocene sea-level fall, which is considered as an important trigger for the emergence of reef

850 islands in the Central Pacific (Dickinson, 2004, 2009; Kench et al., 2014 and references
851 therein). These conglomerates cover unevenly the coral microatoll terraces and the reef flat
852 units and have been interpreted as storm deposits. Their more extensive development during
853 the Holocene compared to modern environments is primarily related to higher sea-level stands
854 and not necessarily to more intense or more frequent storms during this period (Etienne and
855 Terry, 2012). However, the timing of the maximum occurrence of storm deposits that we have
856 reported between 2.2 and 1.5 kyr BP coincides with a peak in accumulation of storm deposits
857 observed between 3.25 and 1.5 kyr BP on the Society Islands and the entire Central South
858 Pacific (Toomey et al., 2013), as well as other Pacific islands such as the Marshall Islands
859 (Kench et al., 2014). The majority of loose reef boulders of several metres that were
860 transported by storm waves onto the reef flat also belong mostly to this time window as their
861 maximum abundance has been reported between 1.7 and 1.1 kyr BP.

862 Mid-late Holocene reef deposits, especially reef flat units as well as conglomerate pavements
863 and accumulations, display an extensive development in the relevant coastal areas and extend
864 partly below modern islets. This suggests that they have played a prominent role in the
865 formation and shaping of modern islands. Based on their distribution, it seems likely that the
866 accumulations of conglomerates, and to a lesser extent of reef flat units, have formed
867 foundations for island initiation through the creation of prominent topographic features that
868 governed or influenced further deposition of sediments. Higher Holocene sea-level stands
869 have been essential in promoting the stranding of extensive spreads of conglomerates on
870 former reef units, which probably correspond to the last vertical accretion stage of the
871 Holocene reef before the sea level reached its present position at 6 kyr BP. Moreover, these
872 thick conglomerate units, including large reworked coral colonies, could correspond to such
873 foundations and were mostly accumulated between 2.2 and 1.5 kyr BP, i.e. during the most
874 recent sea-level fall when sea level was only about 0.2 to 0.4 m higher than modern sea level
875 (Fig. 7). However, this would need to be ascertained in drill cores carried out through modern

876 islets. If confirmed, cyclone activity and high-energy wave events could have initiated, and
877 further controlled, the early development of these islands. The combined role of higher than
878 present sea levels and associated high-energy to storm wave events has been regarded as
879 pivotal in the initiation of other islands, such as Funafuti atoll (Tuvalu; Kench et al., 2018)
880 and the southern Maldives (East et al., 2018). Moreover, it has been demonstrated that
881 Takapoto atoll was gradually formed through the stacking of successive shingle ridges over
882 the last millennium, suggesting that modern islet forms were acquired about 500 to 300 years
883 ago (Montaggioni et al., 2018). This model therefore infers that islands have accreted recently
884 when conglomeratic foundations were emergent and sea level was at its present position.

885

886 *5.2 Importance for future sea-level rise*

887 Geological records of coastal system evolution during past higher and/or rising sea levels
888 provide an important baseline for developing projections regarding the response of modern
889 coastal systems to future sea-level rise. The potential analogues that are currently used are
890 from the Holocene and the Last Interglacial (Woodroffe and Murray-Wallace, 2012; Camoin
891 and Webster, 2015), but neither of these periods appears as a direct analogue for the future.
892 The development, architecture and composition of reef systems are governed by changes in
893 accommodation space, which are mostly controlled by RSL changes and the antecedent
894 topography. Both the amplitude and rates of RSL changes are of prime importance to help
895 forecasting the response of coral reefs and coastal systems to future sea-level change.

896 A key aspect of this study is to document a high-resolution record of coral reef and coastal
897 system responses to mid-late Holocene RSL changes, which is of global significance. The
898 course of mid-late Holocene RSL changes is typified by a succession of episodes of slow sea-
899 level variations separated from each other by extended periods of sea-level stillstands on
900 decadal to centennial time scales (Hallmann et al., 2018). As such, it differs from the
901 predicted sea-level curve for the next decades, which is expected to rise continuously and

902 probably to accelerate sharply in the second part of the current century (IPCC, 2018).

903 However, the mid-late Holocene provides the opportunity to document the response of coral
904 reefs and coastal systems to an increased accommodation space following a sea-level rise of
905 about 1 m in amplitude. The inferred amplitude of RSL changes (~1 m) displays therefore
906 some similarities with ongoing and future sea-level rise (Alley et al., 2007; Church et al.,
907 2013; IPCC, 2018).

908 Rates of mid-late Holocene RSL changes range from a few tens of millimetres per year to 2.5
909 mm/yr and are therefore lower than the predicted rates of sea-level rise by the end of the
910 century, which should range between 5.5 and 10 mm/yr depending on the various scenarios of
911 global warming (IPCC, 2018). In contrast, rates of Holocene sea-level rise before stabilisation
912 of sea level at its present position range from 6 to 10 mm/yr (see review in Camoin and
913 Webster, 2015) are closer to the predicted rates of sea-level rise by the year 2100. However,
914 the more limited accommodation space during most of the Holocene transgression compared
915 to the current situation suggests that this period cannot be seen as a strict analogue of
916 conditions that might prevail for reef development in the future.

917 All studies concerning the timing and processes of island formation during periods of higher
918 sea level, such as the mid-late Holocene, help to better predict the island evolution in the
919 context of global warming and related sea-level rise. However, any prediction must be
920 considered with care due to the different time scales involved, a millennial time scale for
921 island formation vs a decadal/centennial time scale for their future evolution. One could
922 consider in a first analysis that the future evolution of the coastal zones in tropical islands
923 could mimic the mid-late Holocene situation with a more extensive development of reef
924 systems, especially reef flat units, and widespread accumulations of reworked material related
925 to increased cyclone activity and high-energy wave events. The combined effects of these
926 processes could therefore induce another phase of island building in future higher sea-level
927 conditions. However, the growth capacity of coral reefs has decreased sharply over the last

928 decades, mostly due to detrimental factors like sea surface temperature increase, ocean
929 acidification and environmental pollution, and is significantly lower than during the Holocene
930 when ecological conditions were seemingly optimal. A period of enhanced reef development
931 is therefore questionable. The pivotal role of high-energy wave events in a future phase of
932 island formation has been considered (East et al., 2018), but this will be dependent both on the
933 morphology and internal structure of the relevant islands and on the magnitude and frequency
934 of future extreme climate events. A uniform response of tropical islands to future sea-level
935 and climate changes will not occur. A better understanding of this response will require
936 detailed studies regarding reef development as well as island formation and evolution in
937 context of higher and rising sea levels.

938

939 **6. Conclusions**

940 This paper documents in unprecedented detail the impact of RSL changes on reef and coastal
941 development during the mid-late Holocene, a period characterized by slow-rate, low-
942 amplitude and high-frequency sea-level changes. It provides the opportunity to document the
943 response of coral reefs and coastal systems to changing accommodation space in relation to
944 low-amplitude (~1 m) RSL changes. This might help to better assess how these systems might
945 respond to the sea-level rise that is expected by the year 2100.

946 1 - The high-resolution reconstruction of reef geometry, composition and evolution during the
947 mid-late Holocene sheds new light on coral reef responses to low-amplitude, high-frequency
948 RSL changes, at rates ranging from a few tens of millimetres per year up to 2.5 mm/yr. It
949 summarizes the adjustments that reef systems have to make to longer-term changes in
950 accommodation space driven by variations in relative sea level (sea-level rise, stillstand and
951 fall) and therefore helps in the understanding of reef dynamic processes that are of global
952 importance.

953 After the stabilisation of sea level at its present position, the new development of reef systems
954 was initiated by the creation of accommodation space due to a glacio-eustatic sea-level rise
955 from 6.0 to 4.10 kyr BP, most likely sourced from Antarctica, and controlled by the
956 antecedent topography of the islands. A single short-lived sea-level highstand of less than one
957 metre between 4.10 and 3.40 kyr BP is documented. The reversal from rise to fall records the
958 time at which the eustatic signal reduces and GIA (syphoning) becomes dominant, between
959 4.1 and 3.4 kyr BP. Minor sea-level variability probably driven by climatic oscillations has
960 been evidenced during the entire time window, including during the sea-level fall between 3.4
961 and 1.26 kyr BP.

962 Regionally, continuous reef development was maintained throughout the last 6,000 years and
963 typified by the widespread development of microatoll fields and reef flat units. The
964 persistence of reef assemblages displaying similar overall composition and diversity during
965 the whole period and the continuous development of coral microatolls suggest optimal
966 environmental conditions. The facies distribution as well as the lateral extension and shift of
967 facies belts have been governed by variations in accommodation space, which are controlled
968 by changes in relative sea-level and antecedent topography. The recurrent sea-level stillstands,
969 lasting more than a century and up to 250 years, that punctuated the mid-late Holocene sea-
970 level history have played a significant role in the development of dense reef frameworks.

971 2 - The detailed reconstruction of reef development over the last 6,000 years brings valuable
972 information regarding the timing and processes of island formation during periods of higher
973 sea level. It therefore helps predicting how low-lying islands might respond to rising sea
974 levels over the coming decades.

975 The widespread development of mid-late Holocene reef deposits in coastal areas, especially
976 reef flat units and storm conglomerate deposits, suggests that they have played a prominent
977 role in the formation and shaping of modern islands and islets, through the creation of
978 significant topographic features that formed the foundations for island initiation and

979 governed/influenced further deposition of sediments. Further investigations are needed to
980 better unravel the formation of modern islands.

981

982 **Acknowledgements**

983 The authors wish to thank the Polynesian authorities and services for their constant support
984 and assistance, and all the Polynesian companies and friends for their help during field work
985 studies. GM acknowledges support from the Natural Sciences and Engineering Research
986 Council of Canada. ES acknowledges support from the Swiss National Science Foundation
987 (Project 140618).

988 The authors gratefully acknowledge the Editor-in-Chief Jed O. Kaplan and two anonymous
989 reviewers for providing constructive comments, which certainly helped in improving the
990 quality of this paper.

991

992 **Data availability**

993 The data that support the findings of this study are available from the corresponding author
994 upon reasonable request. Measurements of elevations and absolute ages of mid-late
995 Holocene features are available in the data repository PANGAEA:
996 <https://doi.pangaea.de/10.1594/PANGAEA.883846> (Hallmann et al., 2018) and XY (this
997 study).

998

999 **References**

- 1000 Alley, R., Spencer, M., Anandakrishnan, S., 2007. Ice sheet mass balance, assessment,
1001 attribution and prognosis. *Ann. Glaciol.* 46, 1–7.
1002 <https://doi.org/10.3189/172756407782871738>.
- 1003 Bard, E., Hamelin, B., Arnold, M., Montaggioni, L.F., Cabioch, G., Faure, G., Rougerie, F.,
1004 1996. Deglacial sea level record from Tahiti corals and the timing of global meltwater
1005 discharge. *Nature* 382, 241–244. <https://doi.org/10.1038/382241a0>.
- 1006 Becker, M., Meyssignac, B., Letetrel, C., Llovel, W., Cazenave, A., Delcroix, T., 2012. Sea
1007 level variations at tropical Pacific islands since 1950. *Glob. Planet. Chang.* 80–81, 85–98.
1008 <https://doi.org/10.1016/j.gloplacha.2011.09.004>.
- 1009 Blais, S., Guille, G., Guillou, H., Chauvel, C., Maury, R.C., Caroff, M., 2000. Géologie,
1010 géochimie et géochronologie de l'île de Bora Bora (Société, Polynésie Française). *CR Acad.*
1011 *Sci. Paris* 331, 579–585. [https://doi.org/10.1016/S1251-8050\(00\)01456-7](https://doi.org/10.1016/S1251-8050(00)01456-7).
- 1012 Bonneville, A., Le Suavé, R., Audin, L., Clouard, V., Dosso, L., Gillot, P.Y., Janney, P.,
1013 Jordahl, K., Maamaatuaiahutapu, K., 2002. Arago Seamount: The missing hotspot found in
1014 the Austral Islands. *Geology* 30, 1023–1026. [https://doi.org/10.1130/0091-](https://doi.org/10.1130/0091-7613(2002)030<1023:ASTMHF>2.0.CO;2)
1015 [7613\(2002\)030<1023:ASTMHF>2.0.CO;2](https://doi.org/10.1130/0091-7613(2002)030<1023:ASTMHF>2.0.CO;2).
- 1016 Bonneville, A., Dosso, L., Hildenbrand, A., 2006. Temporal evolution and geochemical
1017 variability of the South Pacific superplume activity. *Earth Planet. Sci. Lett.* 244, 251–269.
1018 <https://doi.org/10.1016/j.epsl.2005.12.037>.
- 1019 Botella, A., 2015. Past and Future Sea Level Changes in French Polynesia. MSc. thesis,
1020 University of Ottawa, Canada.
- 1021 Brousse, R., Philippet, J.-C., Guille, G., Bellon, H., 1972. Géochronométrie des Îles Gambier
1022 (Océan Pacifique). *CR Acad. Sci. Paris* 274, 1995.

1023 Cabioch, G., Camoin, G., Montaggioni, L.F., 1999. Post glacial growth history of a French
1024 Polynesian barrier reef tract, Tahiti, central Pacific. *Sedimentology* 46, 985–1000.
1025 <https://doi.org/10.1046/j.1365-3091.1999.00254.x>.

1026 Camoin, G.F., Webster, J.M., 2015. Coral reef response to Quaternary sea-level and
1027 environmental changes: State of the science. *Sedimentology* 62, 401-428.
1028 <https://doi.org/10.1111/sed.12184>.

1029 Camoin, G.F., Gautret, P., Montaggioni, L.F., Cabioch, G., 1999. Nature and environmental
1030 significance of microbialites in Quaternary reefs: the Tahiti paradox. *Sed. Geol.* 126, 271–304.
1031 [https://doi.org/10.1016/S0037-0738\(99\)00045-7](https://doi.org/10.1016/S0037-0738(99)00045-7).

1032 Camoin, G.F., Ebren, Ph., Eisenhauer, A., Bard, E., Faure, G., 2001. A 300,000-yr coral reef
1033 record of sea-level changes, Mururoa Atoll (Tuamotu Archipelago, French Polynesia).
1034 *Palaeogeogr. Palaeoclimatol. Palaeoecol.* 175, 325–341. [https://doi.org/10.1016/S0031-](https://doi.org/10.1016/S0031-0182(01)00378-9)
1035 [0182\(01\)00378-9](https://doi.org/10.1016/S0031-0182(01)00378-9).

1036 Camoin, G.F., Seard, C., Deschamps, P., Webster, J.M., Abbey, E., Braga, J.C., Iryu, Y.,
1037 Durand, N., Bard, E., Hamelin, B., Yokoyama, Y., Thomas, A.L., Henderson, G.M.,
1038 Dussouillez, P., 2012. Reef response to sea-level and environmental changes during the last
1039 deglaciation: Integrated Ocean Drilling Program Expedition 310, Tahiti Sea Level. *Geology*
1040 40, 643–646. <https://doi.org/10.1130/G32057.1>.

1041 Chappell, J., 1983. Evidence for smoothly falling sea level relative to north Queensland,
1042 Australia, during the past 6,000 yr. *Nature* 302, 406–408. <https://doi.org/10.1038/302406a0>.

1043 Church, J.A., Clark, P.U., Cazenave, A., Gregory, J.M., Jevrejeva, S., Levermann, A.,
1044 Merrifield, M.A., Milne, G.A., Nerem, R.S., Nunn, P.D., Payne, A.J., Pfeffer, W.T.,
1045 Stammer, D., Unnikrishnan, A.S., 2013. Sea Level Change. In: Stocker, T.F., Qin, D.,
1046 Plattner, G.-K., Tignor, M., Allen, S.K., Boschung, J., Nauels, A., Xia, Y., Bex, V.,
1047 Midgley, P.M. (Eds.), *Climate Change 2013: The Physical Science Basis. Contribution of*
1048 *Working Group I to the Fifth Assessment Report of the Intergovernmental Panel on Climate*

1049 Change. Cambridge University Press, Cambridge, United Kingdom and New York, NY,
1050 USA, pp. 1137–1216.

1051 Clouard, V., Bonneville, A., 2001. How many Pacific hotspots are fed by deep mantle
1052 plumes? *Geology* 29, 695–698. [https://doi.org/10.1130/0091-](https://doi.org/10.1130/0091-7613(2001)029<0695:HMPHAF>2.0.CO;2)
1053 [7613\(2001\)029<0695:HMPHAF>2.0.CO;2](https://doi.org/10.1130/0091-7613(2001)029<0695:HMPHAF>2.0.CO;2).

1054 Dechnik, B., Webster, J.M., Webb, G.E., Nothdurft, L., Zhao, J.-x., 2017. Successive phases
1055 of Holocene reef flat development: Evidence from the mid- to outer Great Barrier Reef.
1056 *Palaeogeogr. Palaeoclimatol. Palaeoecol.* 466, 221–230.
1057 <https://doi.org/10.1016/j.palaeo.2016.11.030>.

1058 Deschamps, P., Durand, N., Bard, E., Hamelin, B., Camoin, G., Thomas, A., Henderson, G.,
1059 Okuno, J., Yokoyama, Y., 2012. Ice sheet collapse and sea-level rise at the Bølling warming
1060 14,600 yr ago. *Nature* 483, 559–564. <https://doi.org/10.1038/nature10902>.

1061 Detrick, R.S., Crough, S.T., 1978. Island subsidence, hot spots, and lithospheric thinning. *J.*
1062 *Geophys. Res.* 83, 1236–1244. <https://doi.org/10.1029/JB083iB03p01236>.

1063 Dickinson, W.R., 2004. Impacts of eustasy and hydro-isostasy on the evolution and landforms
1064 of Pacific atolls. *Palaeogeogr. Palaeoclimatol. Palaeoecol.* 213, 251–269.
1065 <https://doi.org/10.1016/j.palaeo.2004.07.012>.

1066 Dickinson, W.R., 2009. Pacific atoll living: how long already and until when? *GSA Today* 19,
1067 4–10. <https://doi.org/10.1130/GSATG35A.1>.

1068 Duncan, R.A., McDougall, I., 1974. Migration of volcanism with time in the Marquesas
1069 Islands, French Polynesia. *Earth Planet. Sci. Lett.* 21, 414–420. [https://doi.org/10.1016/0012-](https://doi.org/10.1016/0012-821X(74)90181-2)
1070 [821X\(74\)90181-2](https://doi.org/10.1016/0012-821X(74)90181-2).

1071 Duncan, R.A., McDougall, I., 1976. Linear volcanism in French Polynesia. *J. Volcanol.*
1072 *Geoth. Res.* 1, 197–227. [https://doi.org/10.1016/0377-0273\(76\)90008-1](https://doi.org/10.1016/0377-0273(76)90008-1).

1073 Duncan, R.A., Clague, D.A., 1985. Pacific plate motion recorded by linear volcanic chains,
1074 in: Nairn, A.E.M., Stehli, F.G., Uyeda, S. (Eds.), *The Ocean Basins and Margins*. Springer,
1075 Boston, MA, pp. 89–121.

1076 East, H.K., Perry, C.T., Kench, P.S., Liang, Y., Gulliver, P., 2018. Coral reef island initiation
1077 and development under higher than present sea levels. *Geophys. Res. Lett.* 45, 11265–11274.
1078 <https://doi.org/10.1029/2018GL079589>.

1079 Etienne, S., Terry, J.P., 2012. Coral boulders, gravel tongues and sand sheets: Features of
1080 coastal accretion and sediment nourishment by Cyclone Tomas (March 2010) on Taveuni
1081 Island, Fiji. *Geomorphology* 175–176, 54–65.
1082 <https://doi.org/10.1016/j.geomorph.2012.06.018>.

1083 Fadil, A., Sichoix, L., Barriot, J.-P., Ortéga, P., Willis, P., 2011. Evidence for a slow
1084 subsidence of the Tahiti Island from GPS, DORIS, and combined satellite altimetry and tide
1085 gauge sea level records. *C. R. Geosci.* 343, 331–341.
1086 <https://doi.org/10.1016/j.crte.2011.02.002>.

1087 Fietzke, J., Liebetrau, V., Eisenhauer, A., Dullo, C., 2005. Determination of uranium isotope
1088 ratios by multi-static MIC-ICP-MS: Method and implementation for precise U- and Th-
1089 series isotope measurements. *J. Anal. At. Spectrom.* 20, 395–401.
1090 <https://doi.org/10.1039/B415958F>.

1091 Gabrié, C., Salvat, B., 1985. General features of French Polynesian islands and their coral
1092 reefs, in: Delesalle, B., Galzin, R., Salvat, B. (Eds.), *Proceedings of the 5th International Coral*
1093 *Reef Congress Tahiti*. Volume 1, pp. 1–16.

1094 Galzin, R., Pointier, J.P., 1985. Moorea island, Society archipelago, in: Delesalle, B., Galzin,
1095 R., Salvat, B. (Eds.), *Proceedings of the 5th International Coral Reef Congress Tahiti*. Volume
1096 1, pp. 73–102.

1097 Gischler, E., Hudson, H., Humblet, M., Braga, J., Eisenhauer, A., Isaack, A., Anselmetti, F.,
1098 Camoin, G., 2016. Late Quaternary barrier and fringing reef development of Bora Bora

1099 (Society Islands, south Pacific): first subsurface data from the Darwin type barrier-reef
1100 system. *Sedimentology* 63, 1522–1549. <https://doi.org/10.1111/sed.12272>.

1101 Gischler, E., Hudson, H.J., Humblet, M., Braga, J.C., Schmitt, D., Isaack, A., Eisenhauer,
1102 A., Camoin, G.F., 2019. Holocene and Pleistocene fringing reef growth and the role of
1103 accommodation space and exposure to waves and currents (Bora Bora, Society Islands,
1104 French Polynesia). *Sedimentology* 66, 305–328. <https://doi.org/10.1111/sed.12533>.

1105 Goodwin, I.D., Harvey, N., 2008. Subtropical sea-level history from coral microatolls in the
1106 Southern Cook Islands, since 300 AD. *Mar. Geol.* 253, 14–25.
1107 <https://doi.org/10.1016/j.margeo.2008.04.012>.

1108 Guillou, H., Gillot, P.-Y., Guille, G., 1994. Age (K-Ar) et position des îles Gambier dans
1109 l’alignement du point chaud de Pitcairn (Pacifique Sud). *CR Acad. Sci. Paris* 318, 635–641.

1110 Guillou, H., Maury, R.C., Blais, S., Cotten, J., Legendre, C., Guille, G., Caroff, M., 2005. Age
1111 progression along the Society hotspot chain (French Polynesia) based on new unspiked K-Ar
1112 ages. *Bull. Soc. géol. Fr.* 176, 135–150. <https://doi.org/10.2113/176.2.135>.

1113 Hallmann, N., Camoin, G., Eisenhauer, A., Botella, A., Milne, G.A., Vella, C., Samankassou,
1114 E., Pothin, V., Dussouillez, P., Fleury, J., Fietzke, J., 2018. Ice volume and climate changes
1115 from a 6000 year sea-level record in French Polynesia. *Nat. Commun.* 9, 285.
1116 <https://doi.org/10.1038/s41467-017-02695-7>.

1117 Harmelin-Vivien, M., 1985. Tikehau atoll, Tuamotu archipelago, in: Delesalle, B., Galzin, R.,
1118 Salvat, B. (Eds.), *Proceedings of the 5th International Coral Reef Congress Tahiti. Volume 1*,
1119 pp. 211–268.

1120 Harris, D.L., Webster, J.M., Vila-Concejo, A., Hua, Q., Yokoyama Y., Reimer, P.J., 2015.
1121 Late Holocene sea-level fall and turn-off of reef flat carbonate production: Rethinking bucket
1122 fill and coral reef growth models. *Geology* 43, 175–178. <https://doi.org/10.1130/G35977.1>.

1123 Helfensdorfer, A.M., Power, H.E., Hubble, T.C.T., 2019. Modelling Holocene analogues of

1124 coastal plain estuaries reveals the magnitude of sea-level threat. *Scientific Reports*, 9, 2667.
1125 <https://doi.org/10.1038/s41598-019-39516-4>.

1126 Hopley, D., 1982. *The Geomorphology of the Great Barrier Reef: Quaternary Development of*
1127 *Coral Reefs*. Wiley, New York.

1128 Hopley, D., Smithers, S.G., Parnell, K.E., 2007. *The Geomorphology of the Great Barrier*
1129 *Reef: Development, Diversity, and Change*. Cambridge University Press, New York.

1130 Humblet, M., Hongo, C., Sugihara, K., 2015. An identification guide to some major
1131 Quaternary fossil reef-building coral genera (*Acropora*, *Isopora*, *Montipora*, and *Porites*). *Isl.*
1132 *Arc* 24, 16–30. <https://doi.org/10.1111/iar.12077>.

1133 IPCC, 2018. Masson-Delmotte, V., Zhai, P., Pörtner, H.-O., Roberts, D., Skea, J., Shukla,
1134 P.R., Pirani, A., Moufouma-Okia, W., Péan, C., Pidcock, R., Connors, S., Matthews, J.B.R.,
1135 Chen, Y., Zhou, X., Gomis, M.I., Lonnoy, E., Maycock, T., Tignor, M., Waterfield, T. (Eds.),
1136 *Global Warming of 1.5°C. An IPCC Special Report on the impacts of global warming of*
1137 *1.5°C above pre-industrial levels and related global greenhouse gas emission pathways, in the*
1138 *context of strengthening the global response to the threat of climate change, sustainable*
1139 *development, and efforts to eradicate poverty*. In press.

1140 Jarrard, R.D., Clague, D.A., 1977. Implications of Pacific island and seamount ages for the
1141 origin of volcanic chains. *Rev. Geophys. Space Phys.* 15, 57–76.
1142 <https://doi.org/10.1029/RG015i001p00057>.

1143 Kekeh, M., Akpınar-Elci, M., Allen, M. J., 2020. Sea Level Rise and Coastal Communities,
1144 in: Akhtar, R. (Ed.), *Extreme Weather Events and Human Health*. Springer International
1145 Publishing, Cham, pp. 171–184.

1146 Kench, P.S., Owen, S.D., Ford, M.R., 2014. Evidence for coral island formation during rising
1147 sea level in the central Pacific Ocean. *Geophys. Res. Lett.* 41, 820–827.
1148 <https://doi.org/10.1002/2013GL059000>.

1149 Kench, P.S., McLean, R.F., Owen, S.D., Tuck, M., Ford, M.R., 2018. Storm-deposited coral
1150 blocks: A mechanism of island genesis, Tutaga island, Funafuti atoll, Tuvalu. *Geology* 46,
1151 915–918. <https://doi.org/10.1130/G45045.1>.

1152 Lambeck, K., 1981. Flexure of the ocean lithosphere from island uplift, bathymetry and geoid
1153 height observations: the Society Islands. *Geophys. J. Roy. Astron. Soc.* 67, 91–114.
1154 <https://doi.org/10.1111/j.1365-246X.1981.tb02734.x>.

1155 Lambeck, K., Woodroffe, C.D., Antonioli, F., Anzidei, M., Gehrels, W.R., Laborel, J.,
1156 Wright, A.J., 2010. Paleoenvironmental records, geophysical modeling, and reconstruction of
1157 sea-level trends and variability on centennial and longer timescales, in: Church J.A.,
1158 Woodworth, P.L., Aarup, T., Wilson, W.S. (Eds.), *Understanding sea-level rise and*
1159 *variability*. Wiley-Blackwell, Chichester, pp. 61–121.

1160 Leonard, N.D., Zhao, J.-x., Welsh, K.J., Feng, Y.-x., Smithers, S.G., Pandolfi, J.M., Clark,
1161 T.R., 2016. Holocene sea level instability in the southern Great Barrier Reef, Australia: high-
1162 precision U–Th dating of fossil microatolls. *Coral Reefs* 35, 625–639.
1163 <https://doi.org/10.1007/s00338-015-1384-x>.

1164 Leonard, N.D., Welsh, K.J., Clark, T.R., Feng, Y.x., Pandolfi, J.M. and Zhao, J.x., 2018. New
1165 evidence for "far-field" Holocene sea level oscillations and links to global climate records.
1166 *Earth Planet. Sci. Lett.* 487, 67–73. <https://doi.org/10.1016/j.epsl.2018.02.008>

1167 Lewis, S.E., Wüst, R.A.J., Webster, J.M., Shields, G.A., 2008. Mid-late Holocene sea-level
1168 variability in eastern Australia. *Terra Nova* 20, 74–81. [https://doi.org/10.1111/j.1365-](https://doi.org/10.1111/j.1365-3121.2007.00789.x)
1169 [3121.2007.00789.x](https://doi.org/10.1111/j.1365-3121.2007.00789.x).

1170 Lewis, S.E., Sloss, C.R., Murray-Wallace, C.V., Woodroffe, C.D., Smithers, S.G., 2013.
1171 Postglacial sea-level changes around the Australian margin: a review. *Quat. Sci. Rev.* 74,
1172 115–138. <https://doi.org/10.1016/j.quascirev.2012.09.006>.

1173 Lewis, S.E., Wüst, R.A.J., Webster, J.M., Collins, J., Wright, S.A., Jacobsen, G., 2015. Rapid
1174 relative sea-level fall along north-eastern Australia between 1200 and 800 cal. yr BP: an

1175 appraisal of the oyster evidence. *Mar. Geol.* 370, 20–30.

1176 <https://doi.org/10.1016/j.margeo.2015.09.014>.

1177 McGranahan, G., Balk, D., Anderson, B., 2007. The rising tide: assessing the risks of climate
1178 change and human settlements in low elevation coastal zones. *Environ. Urban.* 19, 17–37.

1179 <https://doi.org/10.1177/0956247807076960>.

1180 McNutt, M.K., Caress, D.W., Reynolds, J., Jordahl, K.A., Duncan, R.A., 1997. Failure of
1181 plume theory to explain midplate volcanism in the southern Austral islands. *Nature* 389, 479–
1182 482. <https://doi.org/10.1038/39013>.

1183 Meltzner, A.J., Woodroffe, C.D., 2015. Coral Microatolls, in: Shennan, I., Long, A.J.,
1184 Horton, B.P. (Eds.), *Handbook of Sea-Level Research*. John Wiley & Sons, Ltd, Chichester,
1185 UK, pp. 125–145.

1186 Meltzner, A.J., Switzer, A.D., Horton, B.P., Ashe, E., Qiu, Q., Hill, D.F., Bradley, S.L.,
1187 Kopp, R.E., Hill, E.M., Majewski, J.M., Natawidjaja, D.H., Suwargadi, B.W., 2017. Half-
1188 metre sea-level fluctuations on centennial timescales from mid-Holocene corals of Southeast
1189 Asia. *Nat. Commun.* 8, 14387. <https://doi.org/10.1038/ncomms14387>.

1190 Meyssignac, B., Becker, M., Llovel, W., Cazenave, A., 2012. An assessment of two-
1191 dimensional past sea level reconstructions over 1950–2009 based on tide gauge data and
1192 different input sea level grids. *Surv. Geophys.* 33, 945–972. [https://doi.org/10.1007/s10712-](https://doi.org/10.1007/s10712-011-9171-x)
1193 [011-9171-x](https://doi.org/10.1007/s10712-011-9171-x).

1194 Milne, G.A., Mitrovica, J.X., 2008. Searching for eustasy in deglacial sea-level histories.
1195 *Quat. Sci. Rev.* 27, 2292–2302. <https://doi.org/10.1016/j.quascirev.2008.08.018>.

1196 Milne, G.A., Gehrels, W.R., Hughes, C.W., Tamisiea, M.E., 2009. Identifying the causes of
1197 sea-level change. *Nat. Geosci.* 2, 471–478. <https://doi.org/10.1038/ngeo544>.

1198 Mitrovica, J.X., Peltier, W.R., 1991. On postglacial geoid subsidence over the equatorial
1199 oceans. *J. Geophys. Res.* 96, 20053–20071. <https://doi.org/10.1029/91JB01284>.

1200 Mitrovica, J.X., Milne, G., 2002. On the origin of late Holocene sea-level highstands within
1201 equatorial ocean basins. *Quat. Sci. Rev.* 21, 2179–2190. <https://doi.org/10.1016/S0277->
1202 3791(02)00080-X.

1203 Montaggioni, L.F., Camoin, G., 1997. Geology of Makatea Island (Tuamotu archipelago,
1204 French Polynesia), in: Vacher, L., Quinn, T.M. (Eds.), *Geology and Hydrogeology of*
1205 *Carbonate Islands*. Elsevier, Amsterdam, pp. 453–474.

1206 Montaggioni, L.F., Salvat, B., Aubanel, A., Eisenhauer, A., Martin-Garin, B., 2018. The mode
1207 and timing of windward reef-island accretion in relation with Holocene sea-level change: A
1208 case study from Takapoto Atoll, French Polynesia. *Geomorphology* 318, 320–335.
1209 <https://doi.org/10.1016/j.geomorph.2018.06.015>.

1210 Neall, V.E., Trewick, S.A., 2008. The age and origin of the Pacific islands: a geological
1211 overview. *Phil. Trans. Roy. Soc. London B Biol. Sci.* 363, 3293–3308.
1212 <https://doi.org/10.1098/rstb.2008.0119>.

1213 Parsons, B., Sclater, J.G., 1977. An analysis of the variation of ocean floor bathymetry and
1214 heat flow with age. *J. Geophys. Res.* 82, 803–827. <https://doi.org/10.1029/JB082i005p00803>.

1215 Perry, C.T., Smithers, S.G., 2011. Cycles of coral reef ‘turn-on’, rapid growth and ‘turn-off’
1216 over the past 8500 years: a context for understanding modern ecological states and
1217 trajectories. *Glob. Change Biol.* 17, 76–86. <https://doi.org/10.1111/j.1365-2486.2010.02181.x>.

1218 Pirazzoli, P.A., Montaggioni, L.F., 1984. Variations récentes du niveau de l’océan et du bilan
1219 hydrologique dans l’atoll de Takapoto (Polynésie Française). *CR Acad. Sci. Paris* 299, 321–
1220 326.

1221 Pirazzoli, P.A., Montaggioni, L.F., 1988. Holocene sea-level changes in French Polynesia.
1222 *Palaeogeogr., Palaeoclimatol., Palaeoecol.* 68, 153–175. <https://doi.org/10.1016/0031->
1223 0182(88)90037-5.

1224 Pirazzoli, P.A., Montaggioni, L.F., Delibrias, G., Faure, G., Salvat, B., 1985. Late Holocene
1225 sea-level changes in the Society Islands and in the northwest Tuamotu atolls, in: Delesalle, B.,

1226 Galzin, R., Salvat, B. (Eds.), Proceedings of the 5th International Coral Reef Congress Tahiti.
1227 Volume 3, pp. 131–136.

1228 Pirazzoli, P.A., Montaggioni, L.F., Salvat, B., Faure, G., 1988. Late Holocene sea level
1229 indicators from twelve atolls in the central and eastern Tuamotus (Pacific Ocean). *Coral Reefs*
1230 7, 57–68. <https://doi.org/10.1007/BF00301642>.

1231 Rashid, R., Eisenhauer, A., Stocchi, P., Liebetrau, V., Fietzke, J., Rüggeberg, A., Dullo, W.-
1232 C., 2014. Constraining mid to late Holocene relative sea level change in the southern
1233 equatorial Pacific Ocean relative to the Society Islands, French Polynesia. *Geochem.*
1234 *Geophys. Geosyst.* 15, 2601–2615. <https://doi.org/10.1002/2014GC005272>.

1235 Roche, R.C., Perry, C.T., Johnson, K.G., Sultana, K., Smithers, S.G., Thompson, A.A., 2011.
1236 Mid-Holocene coral community data as baselines for understanding contemporary reef
1237 ecological states. *Palaeogeogr., Palaeoclimatol., Palaeoecol.* 299, 159–167.
1238 <https://doi.org/10.1016/j.palaeo.2010.10.043>.

1239 Rougerie, F., 1995. Nature et fonctionnement des atolls des Tuamotu (Polynésie Française).
1240 *Oceanol. Acta* 18, 61–78.

1241 Schlanger, S.O., Garcia, M.O., Keating, B.H., Naughton, J.J., Sager, W.W., Haggerty, J.A.,
1242 Philpotts, J.A., Duncan, R.A., 1984. Geology and geochronology of the Line Islands. *J.*
1243 *Geophys. Res.* 89, 11261–11272. <https://doi.org/10.1029/JB089iB13p11261>.

1244 Sloss, C.R., Murray-Wallace, C.V., Jones, B.G., 2007. Holocene sea-level change on the
1245 southeast coast of Australia: a review. *The Holocene* 17, 999–1014.
1246 <https://doi.org/10.1177/0959683607082415>.

1247 Smithers, S.G., Woodroffe, C. D., 2000. Microatolls as sea-level indicators on a mid-ocean
1248 atoll. *Mar. Geol.* 168, 61–78. [https://doi.org/10.1016/S0025-3227\(00\)00043-8](https://doi.org/10.1016/S0025-3227(00)00043-8).

1249 Toomey, M.R., Donnelly, J.P., Woodruff, J.D., 2013. Reconstructing mid-late Holocene
1250 cyclone variability in the Central Pacific using sedimentary records from Tahaa, French
1251 Polynesia. *Quat. Sci. Rev.* 77, 181–189. <https://doi.org/10.1016/j.quascirev.2013.07.019>.

- 1252 Veron, J.E.N., 2000. Corals of the World. Australian Institute of Marine Science and CRR
1253 Qld Pty Ltd, Townsville, Australia, 3 volumes.
- 1254 Wallace, C.C., 1999. Staghorn corals of the world. Museum of Tropical Queensland, CSIRO
1255 Publishing, Collingwood, Australia.
- 1256 Woodroffe, C. D., Murray-Wallace, C. V. 2012. Sea-level rise and coastal change: the past as
1257 a guide to the future. *Quat. Sci. Rev.* 54, 4-11.
1258 <https://doi.org/10.1016/j.quascirev.2012.05.009>.
- 1259 Yamamoto, Y., Ishizuka, O., Sudo, M., Uto, K., 2007. $^{40}\text{Ar}/^{39}\text{Ar}$ ages and palaeomagnetism of
1260 transitionally magnetized volcanic rocks in the Society Islands, French Polynesia: Raiatea
1261 excursion in the upper-Gauss Chron. *Geophys. J. Int.* 169, 41–59.
1262 <https://doi.org/10.1111/j.1365-246X.2006.03277.x>.

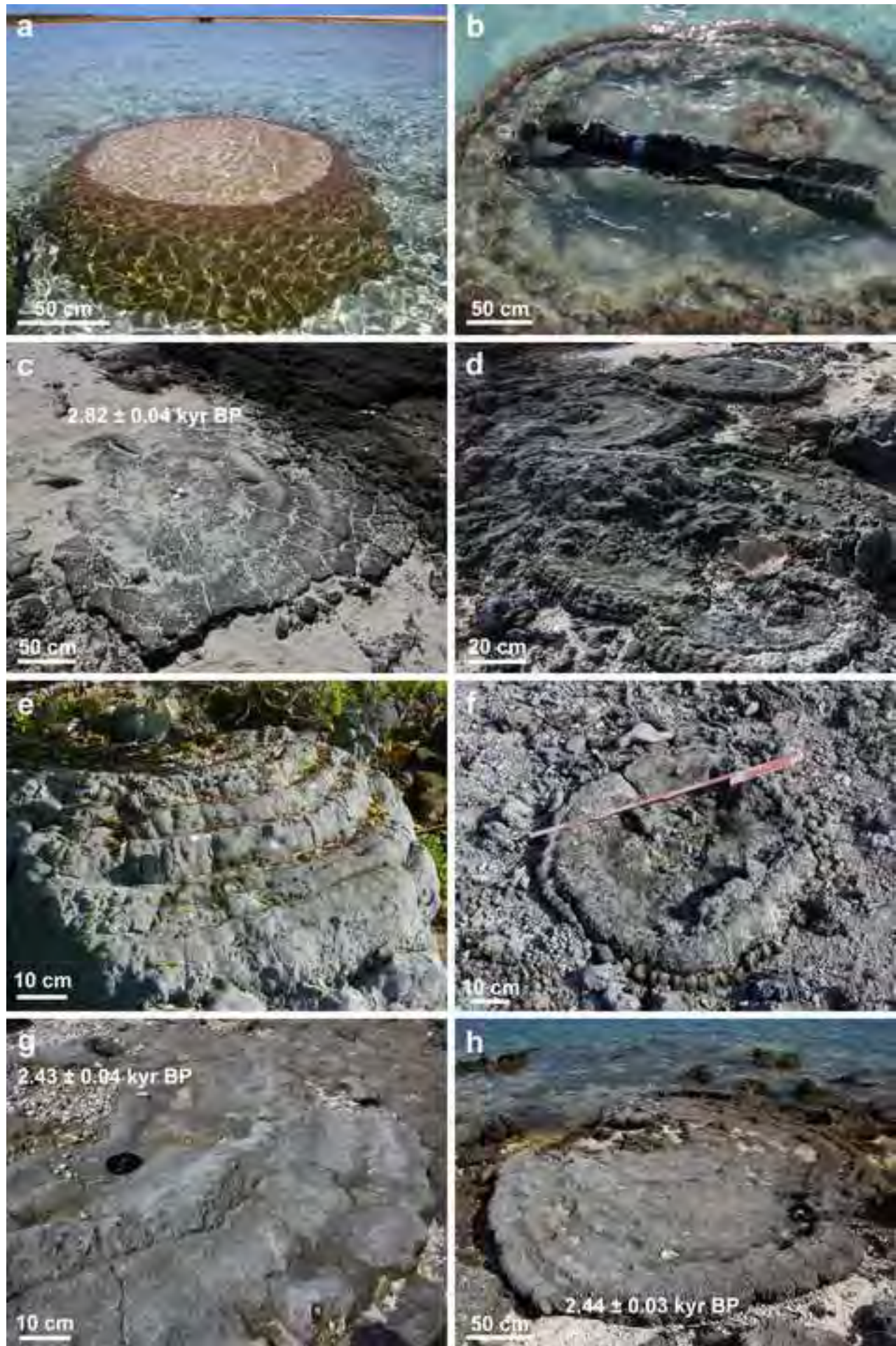


Figure 2

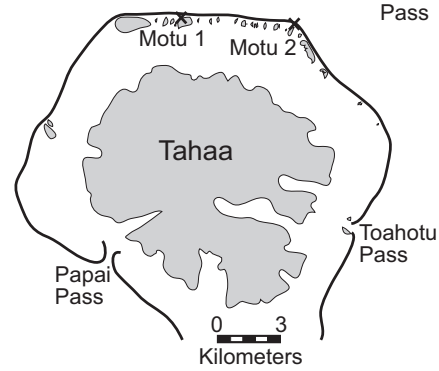
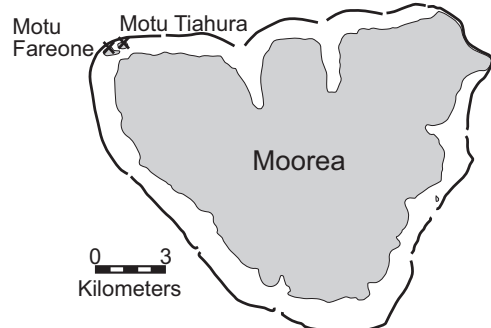
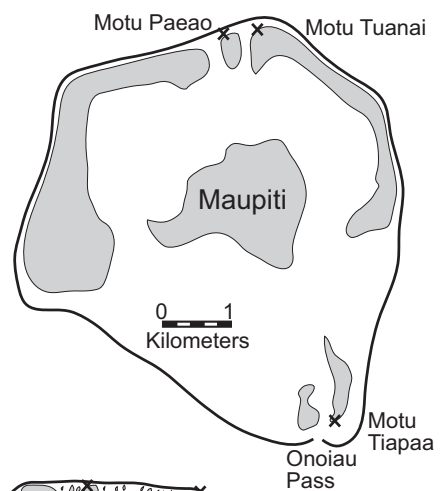
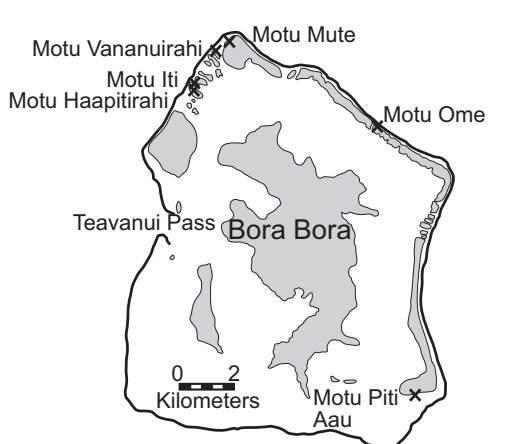
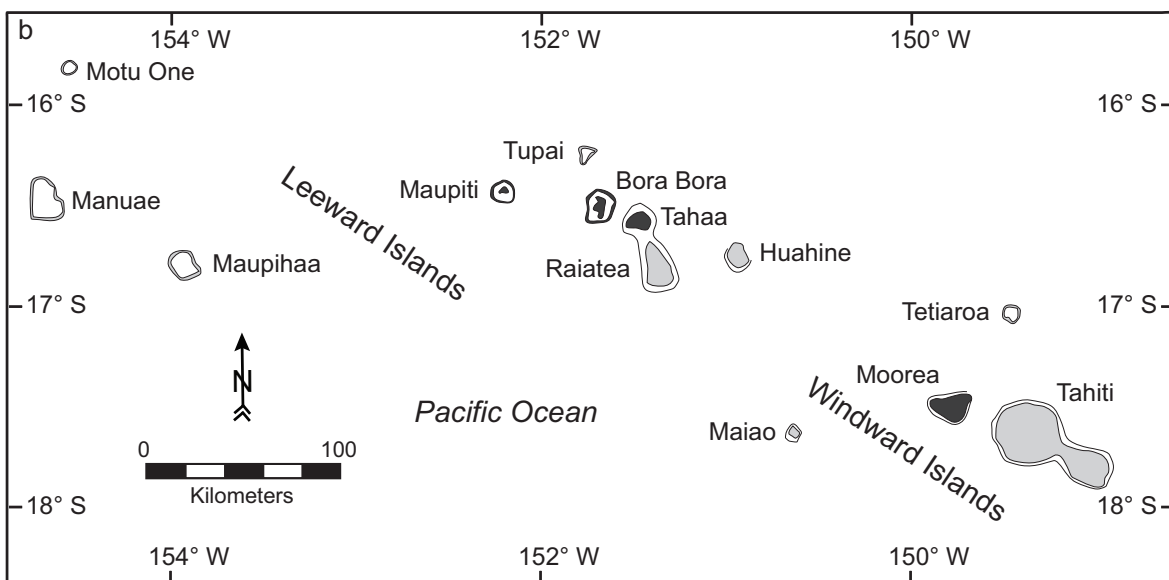
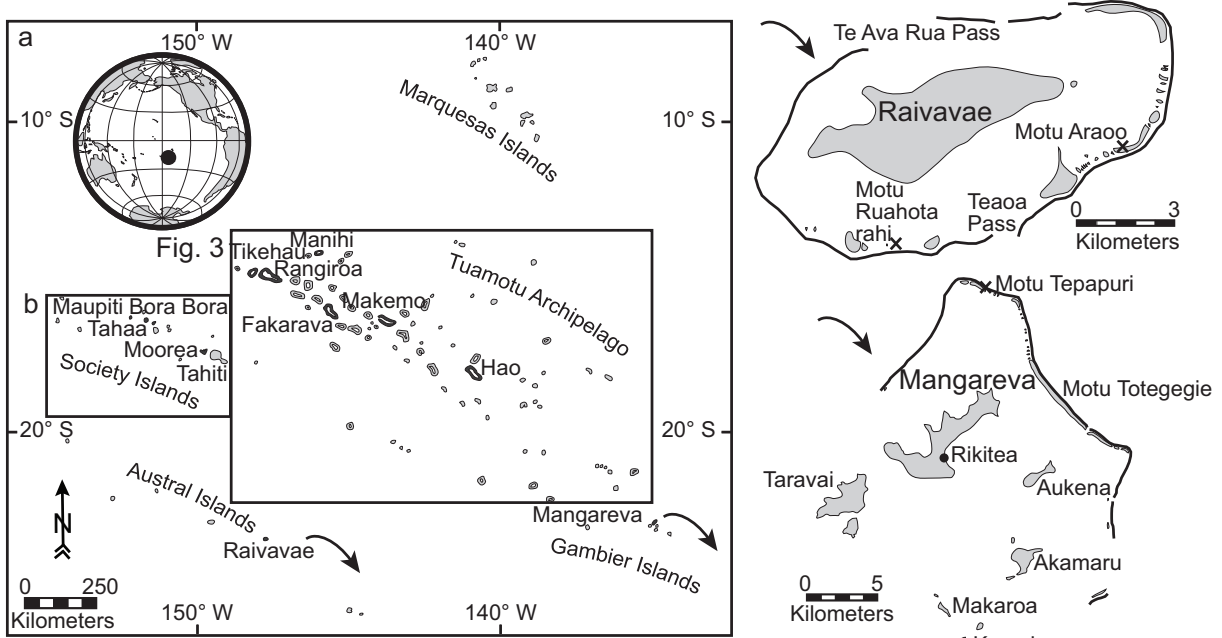


Figure 3

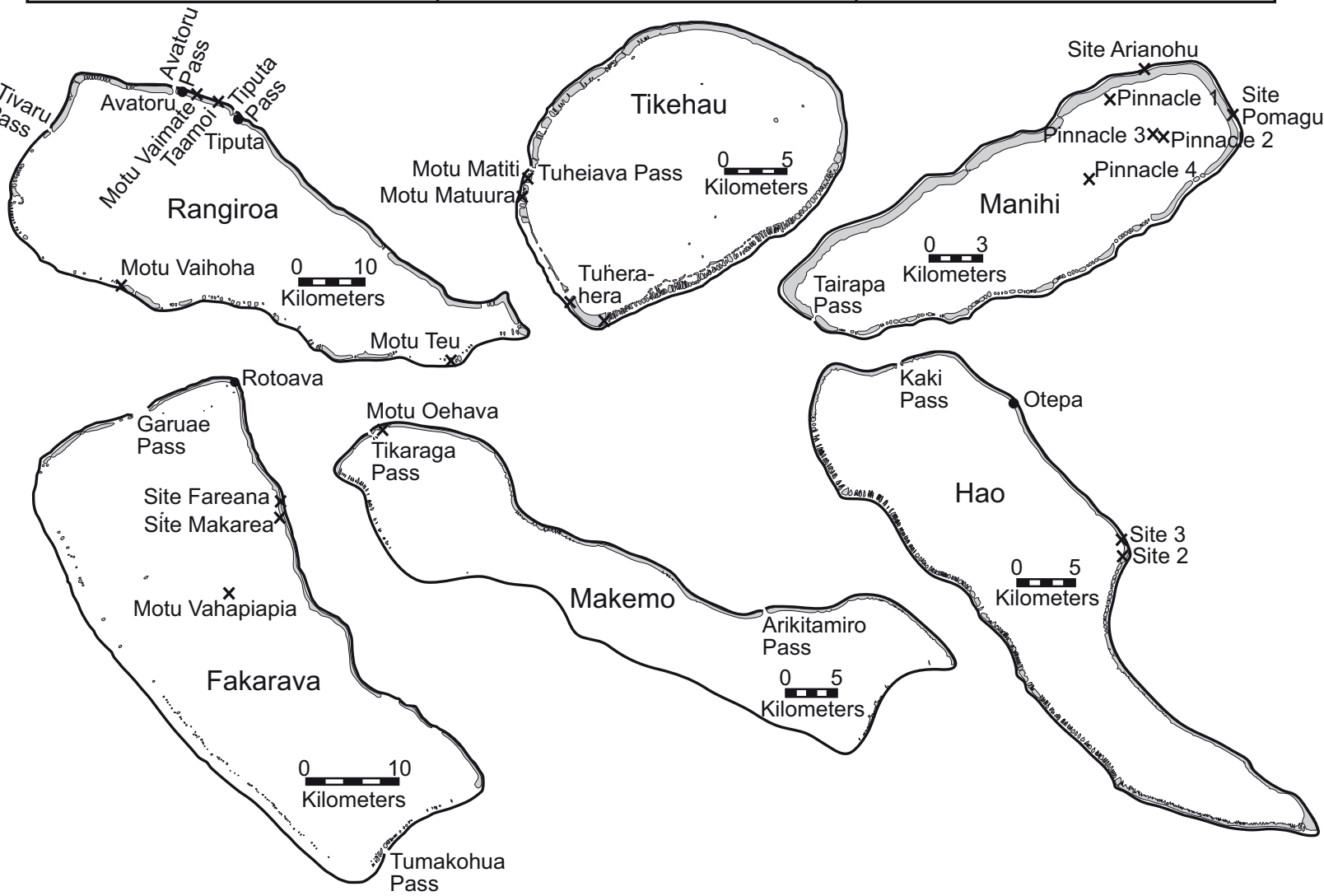
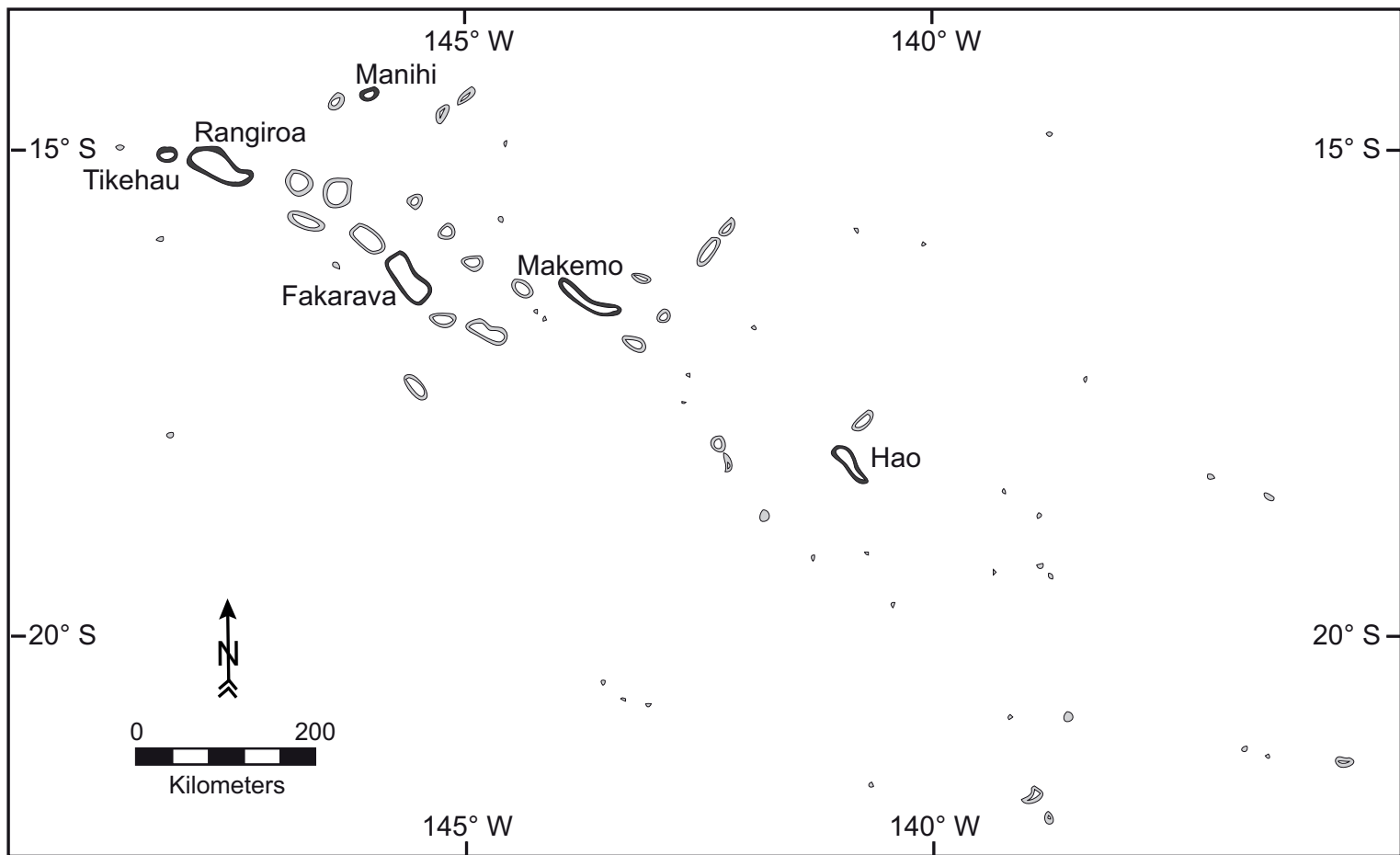
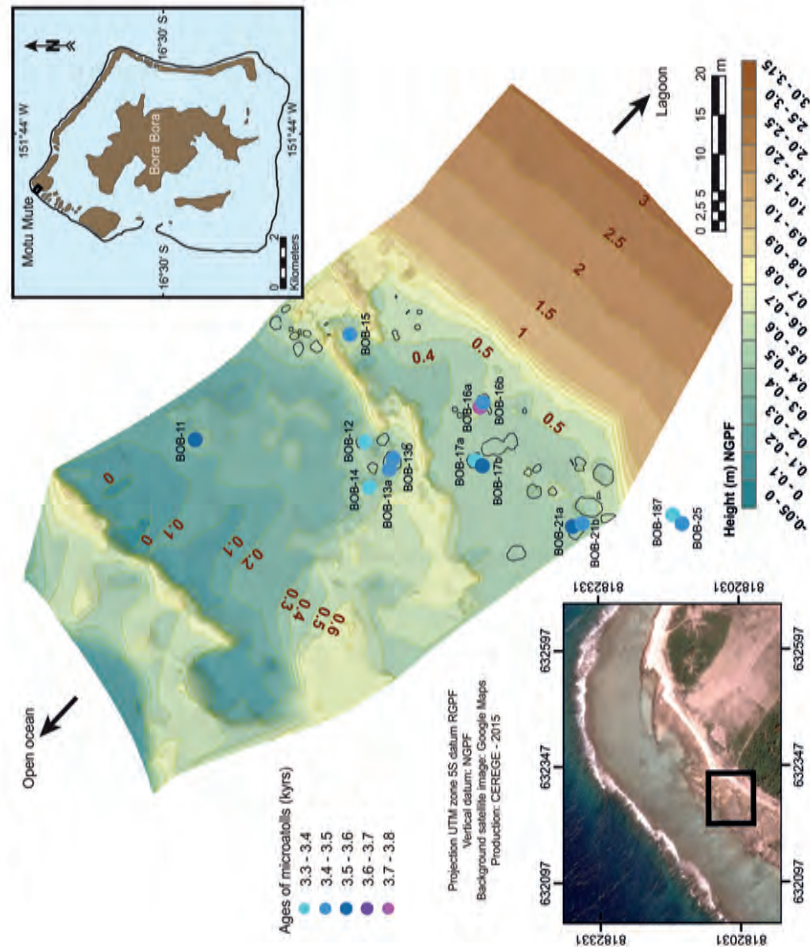


Figure 4



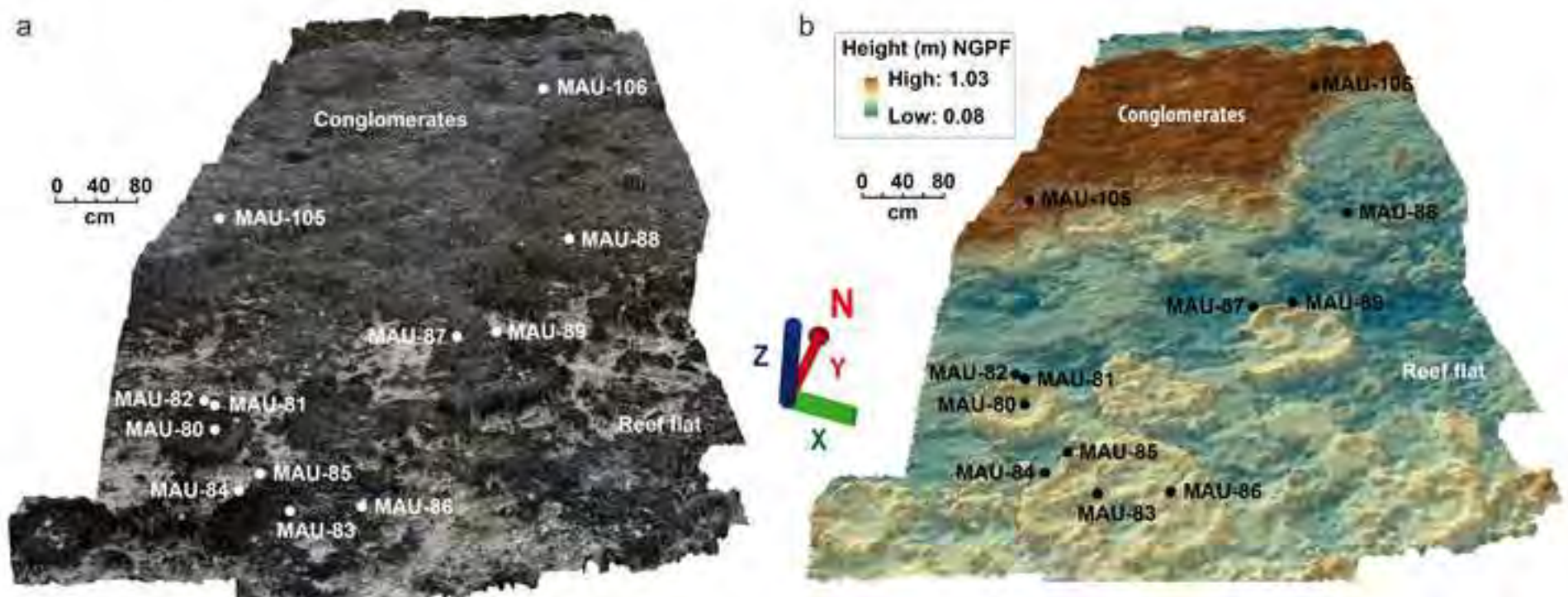
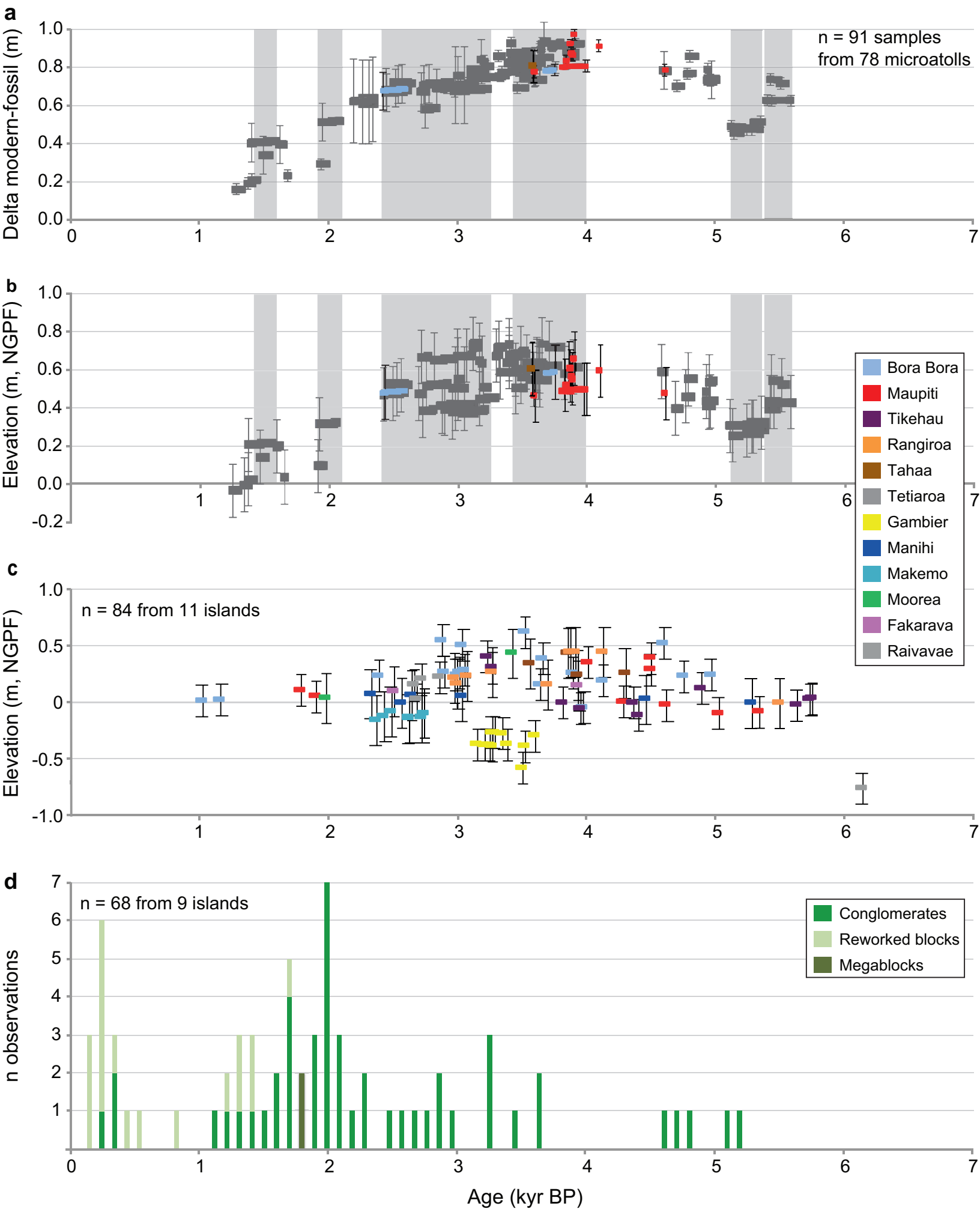


Figure 6



Figure 7



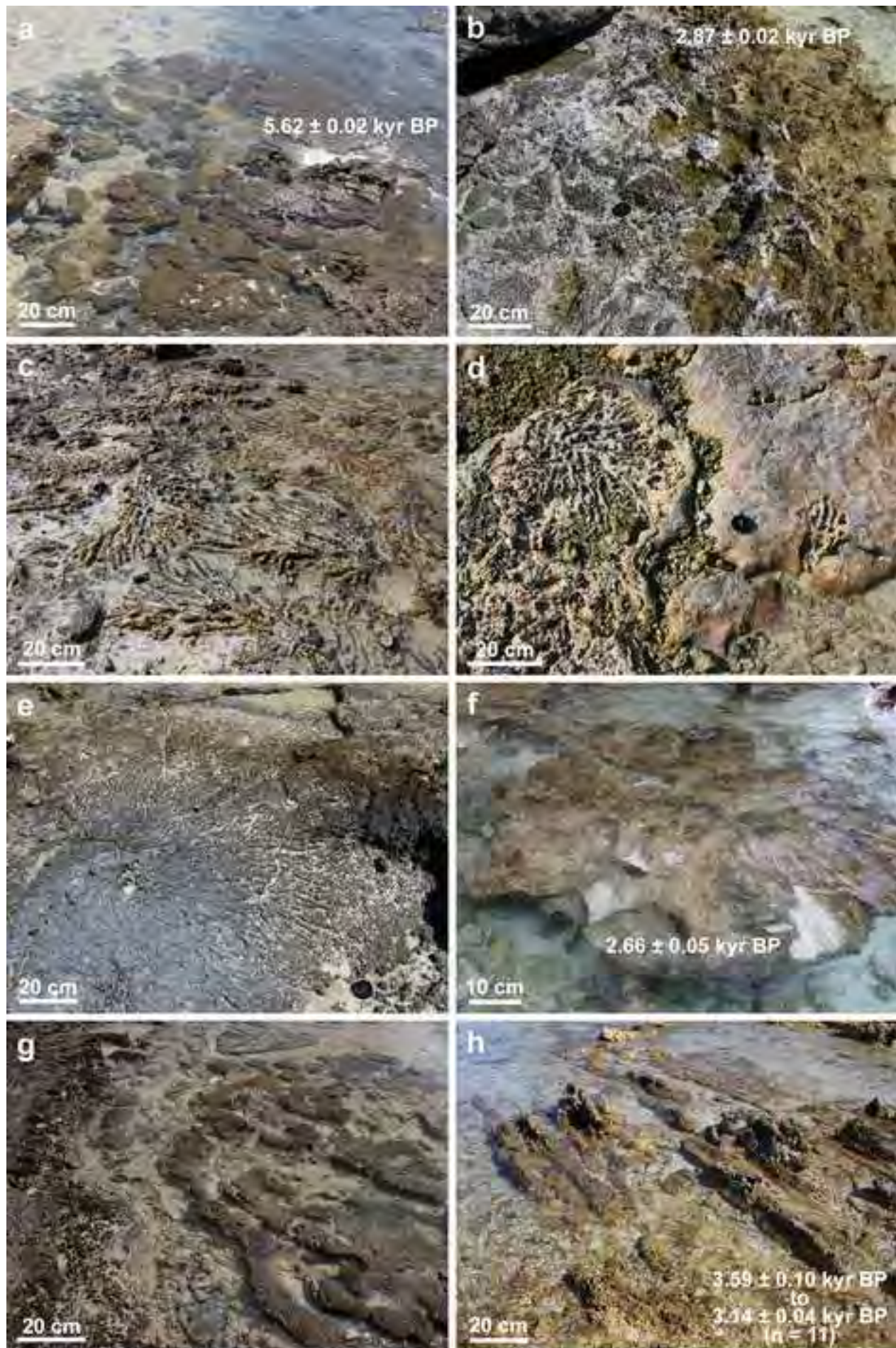






Figure 11

